haematologica
Journal of the Ferrata Storti Foundation

A NOTCH3-CXCL12-driven myeloma-tumor niche signaling axis promotes chemoresistance in multiple myeloma

by Hayley M. Sabol, Cody Ashby, Manish Adhikari, Aric Anloague, Japneet Kaur, Sharmin Khan, Samrat Roy Choudhury, Carolina Schinke, Michela Palmieri, C. Lowry Barnes, Elena Ambrogini, Intawat Nookaew, and Jesus Delgado-Calle

Received: October 10, 2023.
Accepted: February 13, 2024.

Citation: Hayley M. Sabol, Cody Ashby, Manish Adhikari, Aric Anloague, Japneet Kaur, Sharmin Khan, Samrat Roy Choudhury, Carolina Schinke, Michela Palmieri, C. Lowry Barnes, Elena Ambrogini, Intawat Nookaew, and Jesus Delgado-Calle. A NOTCH3-CXCL12-driven myeloma-tumor niche signaling axis promotes chemoresistance in multiple myeloma. Haematologica. 2024 Feb 22. doi: 10.3324/haematol.2023.284443 [Epub ahead of print]

A NOTCH3-CXCL12-driven myeloma-tumor niche signaling axis promotes chemoresistance in multiple myeloma

Hayley M. Sabol[1], Cody Ashby[2,3], Manish Adhikari[1], Aric Anloague[1], Japneet Kaur[1], Sharmin Khan[1], Samrat Roy Choudhury[3,4], Carolina Schinke[3,5], Michela Palmieri[6], C. Lowry Barnes[7], Elena Ambrogini[6], Intawat Nookaew[2,3], and Jesus Delgado-Calle[1,3*]

[1]Physiology and Cell Biology, University of Arkansas for Medical Sciences, Little Rock, AR, US.

[2]Department of Biomedical Informatics, University of Arkansas for Medical Sciences, Little Rock, AR, US. [3]Winthrop P. Rockefeller Cancer Institute, University of Arkansas for Medical Sciences, Little Rock, AR, US. [4]Pediatric Hematology-Oncology, Arkansas Children's Research Institute, University of Arkansas for Medical Sciences, Little Rock, AR, 72202, US. [5]Myeloma Center; University of Arkansas for Medical Sciences, Little Rock, AR, US. [6]Division of Endocrinology and Metabolism, Center for Osteoporosis and Metabolic Bone Diseases and Center for Musculoskeletal Disease Research, University of Arkansas for Medical Sciences and Central Arkansas Veterans Healthcare System, Little Rock, AR, US. [7]Department of Orthopedic Surgery; University of Arkansas for Medical Sciences, Little Rock, AR, US.

Author contributions

J.D.C. conceived and supervised the project. H.M.S, C.A., C.S., and J.D.C. designed the experiments. H.M.S., C.A., M.A., A.A., J.K., S.K., S.R.C., M.P., C.L.B., I.N., and E.A. performed the experiments and/or collected data. H.M.S., C.A., I.N., and J.D.C. contributed to

the data analysis and interpretation. J.D.C and H.M.S. wrote the manuscript. All authors reviewed the manuscript.

Running head: NOTCH3 and chemoresistance in multiple myeloma

Keywords: multiple myeloma, Notch, Bortezomib, bone, chemoresistance

***Corresponding author:** Jesús Delgado-Calle, Ph.D., Department of Physiology and Cell Biology, University of Arkansas for Medical Sciences, 4301 W. Markham St. Little Rock, AR 7220,5, E-mail: jdelgadocalle@uams.edu, Office: +1-501-686-7668; ORCID: 0000-0002-2083-2774

Data sharing statement. The IA15 datasets used for the analyses described in this work were downloaded from the Multiple Myeloma Research Foundation CoMMpass (MMRF CoMMpass [SM] (Relating Clinical Outcomes in MM to Personal Assessment of Genetic Profile) study (www.themmrf.org)) researcher gateway. Other non-public datasets used and analyzed during the current study are available from the corresponding author upon reasonable request.

Abstract word count: 200

Main text count: 4000

Number of figures and tables: 7 main figures and 13 supplementary files

References: 39

Acknowledgments: The authors would like to acknowledge the services provided by the TBAPS of the UAMS Winthrop P. Rockefeller Cancer Institute and the MMRF for providing the CoMMpass IA15 dataset. These data were generated as part of the Multiple Myeloma Research Foundation Personalized Medicine Initiatives (https://research.themmrf.org and www.themmrf.org). The authors thank Dr. Onal for her assistance with CRISPR NOTCH3 activation and sgRNA design.

Funding: This work was supported by the National Institutes of Health (NIH) R37CA251763, R01CA209882, R01CA241677 to J.D.C., P20GM125503 to J.D.C and I.N., and F31CA284655 to H.M.S., the UAMS Musculoskeletal Hub Award to J.D.C. and I.N., the UAMS Translational Research Institute (TRI), grant KL2 TR003108 through the National Center for Advancing Translational Sciences of the NIH to C.A., and the UAMS Winthrop P. Rockefeller Cancer Institute Seeds of Science Award and Voucher Program awarded to J.D.C.

Disclosure of Conflicts of Interest: The authors have declared that no conflict of interest exists.

Abstract

Multiple myeloma (MM) remains incurable due to disease relapse and drug resistance. Notch signals from the tumor microenvironment (TME) confer chemoresistance, but the cellular and molecular mechanisms are not entirely understood. Using clinical and transcriptomic datasets, we found that *NOTCH3* is upregulated in $CD138^{+}$ cells from newly diagnosed MM (NDMM) patients compared to healthy individuals and increased in progression/relapsed MM (PRMM) patients. Further, NDMM patients with high *NOTCH3* expression exhibited worse responses to Bortezomib (BOR)-based therapies. Cells of the TME, including osteocytes, upregulated *NOTCH3* in MM cells and protected them from apoptosis induced by BOR. NOTCH3 activation ($NOTCH3^{OE}$) in MM cells decreased BOR anti-MM efficacy and its ability to improve survival in *in vivo* myeloma models. Molecular analyses revealed that NDMM and PRMM patients with high NOTCH3 exhibit CXCL12 upregulation. TME cells upregulated CXCL12 and activated the CXCR4 pathway in MM cells in a NOTCH3-dependent manner. Moreover, genetic or pharmacologic inhibition of CXCL12 in $NOTCH3^{OE}$ MM cells restored sensitivity to BOR regimes *in vitro* and in human bones bearing $NOTCH3^{OE}$ MM tumors cultured *ex vivo*. Our clinical and preclinical data unravel a novel NOTCH3-CXCL12 pro-survival signaling axis in the TME and suggest that osteocytes transmit chemoresistance signals to MM cells.

Introduction

Multiple myeloma (MM) is a hematological cancer characterized by the accumulation of malignant plasma cells in the bone marrow and the overproduction of monoclonal proteins (M-proteins). First-line therapy in MM includes proteasome inhibitors, such as Bortezomib (BOR), administered alone or in combination regimens.[1] Despite high response rates to BOR-based therapies, MM remains incurable due to the development of chemoresistance and disease recurrence after transient remissions.

Although MM cells exhibit genetic and molecular heterogeneity, they depend highly on the bone marrow niche. MM cells localize in specialized niches in the marrow where tumor microenvironment (TME) cells promote their proliferation and allow them to escape anti-MM therapies by promoting *de novo* chemoresistance.[2-4] Notch signaling activation downstream of the four NOTCH (1-4) receptors in MM cells plays a critical role in transforming the bone marrow into a permissive niche for MM progression and chemoresistance.[5, 6] Pharmacologic pan-inhibition of Notch in the TME induces apoptosis in MM cells and enhances sensitivity to chemotherapy.[6, 7] Notch signals from stromal cells contribute to *de novo* drug resistance to proteasome inhibitors in MM cells.[8] Yet, the role of other TME cells and how MM cells integrate and execute TME Notch signals are not completely understood.

Prior studies have focused on NOTCH1 or 2, as they are expressed at relatively higher levels than *NOTCH3* or *4* in NDMM patients.[9] However, we recently reported that 30% of NDMM patients exhibit *NOTCH3* expression levels comparable to *NOTCH1* or *NOTCH2*.[9] Moreover, we showed that osteocytes, the most abundant bone cells,[10] rapidly upregulate *NOTCH3* expression in MM cells,[9] emphasizing the need to understand the role of NOTCH3 in MM further. In this study, we describe a novel NOTCH3-CXCL12 signaling axis of TME-mediated

chemoresistance and identify the osteocyte as a new TME cell capable of influencing MM therapeutic responses to BOR-based regimes.

Methods

Study population. The mRNA expression of NOTCH receptors was studied in $CD138^+$ plasma cells from a previously described institutional cohort of newly diagnosed MM (NDMM) patients (n=52; t(4;14=8; t(11;14)=10; t(14;16)=9; t(14;20)=6; D1=12; D2=7) and age-matched healthy donors (n=4).[11] To study the impact of *NOTCH3* on the transcriptome and clinical outcomes of MM patients, we obtained clinical and gene expression data from NDMM patients from the Multiple Myeloma Research Foundation (MMRF) CoMMpass registry (NCT01454297, version IA15).

Bioinformatic analyses. Gene expression and mutation analyses are described in **Supplementary Methods**.

Cell culture. MM-osteocyte (5:1) or MM-stroma (5:1) co-cultures were established as described before.[9, 12] Co-cultures were treated with Plerixafor (25uM), BOR (3nM), VRd (BOR: 2nM, Lenalidomide: 1uM, Dexamethasone: 10nM) and refreshed every 24h. Cell characteristics, reagents, and methods for apoptosis/proliferation assays are described in **Supplementary Methods**.

Gene expression. Methods to quantify mRNA (qPCR) and protein expression (Western Blot and ELISA) are described in **Supplementary Methods**.

Genetic inhibition/activation in MM cells. Methods used to manipulate *NOTCH3/CXCL12* expression are described in **Supplementary Methods**.

Ex vivo organ cultures. Ex vivo MM-murine bone organ cultures were established as described before.[12] Ex vivo MM-human bone organ cultures were established with human cancellous bone fragments similar in size obtained from femoral heads discarded after hip arthroplasty (see **Supplementary Methods** for details).

Animal studies. 7-week-old immunodeficient littermate NSG female and male mice were injected intravenously with $5x10^5$ OPM2-Scr MM cells, OPM2-Notch3^{OE} MM cells, or saline. Equal numbers of female and male mice were used per group. After one week, mice were randomized based on tumor burden and bone disease to two groups (1) vehicle (saline) or (2) 0.1mg/kg BOR (i.p.) 5x/wk for 3 weeks. To assess survival, the health of mice was monitored daily, and mice were euthanized at first sign of back leg paralysis. The sample size was calculated based on previous studies.[13, 14] MicroCT analyses were performed as shown before.[12, 14]

Statistics. Data were analyzed using GraphPad (GraphPad Software Inc, San Diego, CA, USA). Differences in means were analyzed using a combination of unpaired *t*-test, One-Way, or Two-Way ANOVA tests, followed by pairwise multiple comparisons (Tukey post hoc test). Values were reported as means ± SD. P values ≤ 0.05 were considered statistically significant. Data analysis was performed in a blinded fashion.

Study Approvals. All procedures involving animals were performed in accordance with guidelines issued by the University of Arkansas for Medical Sciences IACUC (protocol #2022200000489). Collection and de-identification of human bone samples was coordinated by the UAMS Winthrop P. Rockefeller Cancer Institute TBAPS and approved by the UAMS IRB (protocol # 262940). All participants provided written, informed consent before study procedures occurred, with continuous consent ensured throughout participation. NDMM patients and healthy

donors were consented with IRB approval (protocol IRB #260284) for bone marrow aspirates for $CD138^+$ cell selection.

Results

***NOTCH3* expression is increased in newly diagnosed patients (NDMM) by a non-mutational, TME cell-dependent mechanism**. To investigate the integration of Notch signals by MM cells, we first compared the expression of the NOTCH receptors in $CD138^+$ plasma cells using an institutional cohort of NDMM patients of major molecular MM subgroups, including primary translocations t(4;14), t(11;14), t(14;16) and t(14:20), hyperdiploid subgroups D1 and D2, and age-matched healthy donors (**Figure 1A**). We found no differences in the expression of *NOTCH1* or *NOTCH2* in NDMM patients compared to healthy donors, except for a *NOTCH2* upregulation detected in the t(14;16) MM subgroup. *NOTCH4* was decreased in all the MM subgroups, except the t(4;14) MM subgroup. In contrast, *NOTCH3* expression was elevated in all NDMM subgroups, although it did not reach statistical significance in the t(14;16) subgroup. To understand the mechanisms behind *NOTCH3* upregulation in NDMM, we next mined the MMRF CoMMpass cohort dataset to investigate whether *NOTCH3* expression levels in $CD138^+$ plasma cells from NDMM patients correlated with gain- or loss-of-function mutations in the *NOTCH3* gene. We identified several mutations in the *NOTCH3* gene (**Supplementary Table 1**) but did not find an association with *NOTCH3* expression (**Figure 1B**). In addition, we investigated the presence of *NOTCH3* mutations in a panel of 69 human MM cell lines and identified only one cell line, FLAM76 (t11;14), with a frameshift mutation (AGGGG/AGGG). Next, we investigated if constituents of the TME upregulate *NOTCH3* in MM cells. As shown before,[9] co-culture with osteocytes upregulated *NOTCH3* and increased the expression of the

Notch target gene *HES1* in several murine and human MM cell lines (**Supplementary Figure 1A-C**). In contrast, no changes were detected in *NOTCH1*, *2*, or *4*. Like osteocytes, co-culture with stromal cells, another important cellular component of the MM-TME,[2] selectively upregulated *NOTCH3* expression and activated Notch signaling in MM cells (**Supplementary Figure 1D-F)**. Together, these data support that non-mutational, TME cell-dependent NOTCH3 activation occurs in specialized niches in the bone marrow of NDMM patients.

***NOTCH3* expression correlates with worse responses to Bortezomib (BOR)-based therapies in NDMM patients.** Further bioinformatic mining of the CoMMpass cohort revealed that NDMM patients with high *NOTCH3* expression exhibited upregulation and enrichment in genes associated with processes involved in chemoresistance, including *Responses to drugs* (**Figure 2A**) and *Cell-adhesion pathways* (**Figure 2B**). Moreover, gene set enrichment analysis (GSEA) revealed that the transcriptome of high *NOTCH3* NDMM patients is enriched in genes associated with poor responses to BOR therapy (**Figure 2C**).[15] Poised by these observations, we next investigated if high expression levels of *NOTCH3* are associated with poor prognosis in NDMM patients. No significant correlations were observed between the expression of *NOTCH3* and OS or PFS (**Supplementary Figure 2A-B**). However, after stratification by therapy (combined graph is shown in **Supplementary Figure 2C**), we observed that NDMM patients with high *NOTCH3* had significantly worse PFS when receiving BOR-based therapies vs. other therapies not including BOR (**Figure 2D**). In contrast, NDMM patients with low *NOTCH3* levels exhibited similar PFS regardless of the therapy received. Next, we rationalized that if $CD138^+$ MM cells expressing high *NOTCH3* are chemoresistant, the expression of *NOTCH3* should increase in PRMM patients. Consistent with this notion, we found an increase in *NOTCH3* expression in PRMM patients using paired diagnosis-relapse samples of MM patients included in

the CoMMpass cohort (**Figure 2E**). These results suggest that NOTCH3-regulated transcriptional reprogramming of MM cells promotes drug resistance to BOR-based therapies and associates with poor clinical outcomes.

NOTCH3 signaling mediates TME-mediated BOR chemoresistance in MM cells. To investigate the impact of NOTCH3 signaling on drug resistance to BOR-based therapies, we selected murine 5TGM1 and human U266 MM cells, which exhibit higher levels of NOTCH3 expression/activation,[9] and human OPM2 MM cells, with lower NOTCH3 levels (**Supplementary Figure 3A**), and determined that BOR therapy does not affect NOTCH expression in these cell lines (**Supplementary Figure 3B**). Then, we knocked down *NOTCH3* (*NOTCH3*^{KD}) in 5TGM1[9] and U266 MM cells (**Supplementary Figure 3C**) and established co-cultures with cells of the TME (**Figure 3A**). Control (Scr) and *NOTCH3*^{KD} MM cells cultured alone exhibited similar apoptotic responses to BOR and the triple regime VRd (BOR+dexamethasone+lenalidomide), frequently used in induction therapy for NDMM. Co-culture with osteocytes decreased by ~50% the apoptosis induced by BOR or VRd in control MM cells, while this protection was lost in Notch3^{KD} MM cells (**Figure 3A-B**). Second, we used CRISPR-mediated transcriptional activation from the endogenous *NOTCH3* loci to promote a more physiological activation of NOTCH3 in OPM2 MM cells (*NOTCH3*^{OE} cells) while permitting further *NOTCH3* regulation by the TME (**Supplementary Figure 3D**). NOTCH3 activation did not alter the anti-MM efficacy of these therapies in MM cells cultured alone but enhanced the pro-survival effects of osteocytes in *in vitro* co-cultures exposed to BOR or VRd (**Figure 3C**). Similar responses to *NOTCH3* inhibition/activation in MM cells exposed to BOR or VRd were also observed in co-cultures with stromal cells (**Supplementary Figures 4A-C**).

Co-culture with osteocytes or genetic manipulation of *NOTCH3* did not affect the baseline levels of apoptosis in MM cells cultured in the absence of BOR (**Supplementary Figures 4D-E**).

Next, we injected Scr and *NOTCH3*^{OE} OPM2 MM cells in immunodeficient mice and treated them with BOR after the tumors engrafted. BOR decreased tumor progression, reduced tumor burden (~60%), and improved survival in mice injected with control MM cells (**Figure 4A-C**). In contrast, BOR only reduced tumor burden by 23% in mice bearing *NOTCH3*^{OE} MM cells and had no impact on survival. Lastly, to assess the effects of *NOTCH3* inhibition on responses to BOR-based therapies, we established *ex vivo* MM-bone organ cultures (**Figure 4D**), a system that recapitulates the spatial dimension, cellular diversity, and molecular networks of the TME in a controlled setting.[16] Scr or *NOTCH3*^{KD} MM cells were allowed to colonize calvarial bones, treated with BOR, and MM-secreted paraprotein levels were quantified in the media to assess tumor growth (**Figure 4E-F** and **Supplementary Figures 5A and C**). BOR exhibited higher anti-MM efficacy in bones bearing 5TGM1 or U266 *NOTCH3*^{KD} MM cells compared to Scr MM cells (**Figure 4E-F**). Similarly, treatment of bones bearing 5TGM1 *NOTCH3*^{KD} MM cells with VRd resulted in better tumor reduction compared to bones bearing control 5TGM1 tumors (**Supplementary Figure 5B**). Together, this set of experiments supports that NOTCH3 integrates TME-mediated Notch signals in MM cells and confers chemoresistance/sensitivity to BOR-based therapies.

Because we previously reported that NDMM patients with *NOTCH3* have a gene signature consistent with increased osteoclastogenic potential,[9] we examined the impact of NOTCH3 activation on MM-induced bone disease. We found that *NOTCH3*^{OE} MM tumors led to greater reductions in cancellous bone mass and higher levels of the bone resorption biomarker CTX compared to control tumors (**Supplementary Figure 6A-C**), but no differences were detected in

the levels of the bone formation marker P1NP (**Supplementary Figure 6D**). BOR therapy improved cancellous bone mass and P1NP and reduced CTX in mice bearing control MM cells, but had no effect on *NOTCH3*^{OE} MM-bearing mice. Consistent with increased MM osteoclastogenic potential, *NOTCH3*^{OE} MM cells expressed higher mRNA levels of *RANKL*, which were further enhanced by co-culture with osteocytes or stromal cells (**Supplementary Figure 6E**).

NOTCH3 transcriptional reprogramming increases the expression of CXC chemokines in MM cells. To determine the molecular mechanism(s) by which TME-mediated NOTCH3 signaling dictates responses to BOR-based therapies in MM cells, we compared the transcriptome of NDMM patients with high vs. low *NOTCH3* expression (**Supplementary Figure 7**). We found enrichment in GO terms related to *Chemokine signaling*, *CXCR chemokine signaling*, *Chemotaxis*, and *Cell adhesion* (**Supplementary Figure 7A-C**), and upregulation of *Cytokine-cytokine receptor interaction*, *Chemokine signaling pathways*, and *Cell Adhesion Molecules* pathways in NDMM patients with high *NOTCH3* expression (**Figure 5A**). Moreover, several members of the CXC chemokine family were upregulated in NDMM patients with high *NOTCH3* (**Supplementary Figure 7D**). We focused on *CXCL12* because it has been previously linked to cell adhesion-mediated drug resistance in MM.[17, 18] We found a strong positive correlation between *CXCL12* and *NOTCH3* expression in NDMM and PRMM patients (**Figure 5B**). Similar to *NOTCH3*, the expression of *CXCL12* also increased in PRMM patients compared to levels at diagnosis (**Figure 5C**). Additionally, we mined a previously published single-cell RNAseq data set of CD138^{+} plasma cells from PRMM patients[19] and found colocalization of *NOTCH3* and *CXCL12* expression in a subset of CD138^{+} plasma cells from patients with primary refractory MM (**Supplementary Figure 8**). Based on this clinical data, we hypothesized

that TME-mediated NOTCH3 signaling increases *CXCL12* expression in MM cells. Osteocytes increased the expression of *CXCL12* in murine and human MM cells. This increase was prevented in *NOTCH3*^{KD} cells and further increased in *NOTCH3*^{OE} MM cells (**Figure 5D-F**). A similar regulation of *CXCL12* by NOTCH3 was seen in co-cultures with stromal cells (**Supplementary Figure 9**). Together, these clinical and cellular data demonstrate that NOTCH3 signaling regulates *CXCL12* expression in MM cells.

Autocrine CXCL12-CXCR4 signaling mediates NOTCH3-induced chemoresistance in MM cells. Next, we investigated the contribution of CXCL12 to the NOTCH3-mediated acquired chemoresistance triggered by the TME. We found that TME osteocytes activated NOTCH3 signaling by cleaving NICD3, but not NICD1 or 2 (**Supplementary Figure 10**) and increased the phosphorylation of the CXCL12 receptor CXCR4 and the downstream targets ERK 1/2 and AKT in MM cells. These effects were fully prevented in *NOTCH3*^{KD} and enhanced in *NOTCH3*^{OE} MM cells (**Figure 6A-B** and **Supplementary Figure 11**), indicating that CXCL12-CXCR4 signaling in MM cells depends on NOTCH3 signals. To further explore the role of CXCL12-CXCR4 signaling on responses to BOR-based therapies, we first employed Plerixafor, a selective inhibitor of CXCR4. Plerixafor fully restored sensitivity to BOR and VRd in *NOTCH3*^{OE} MM cells co-cultured with osteocytes or stromal cells (**Figure 6C-D** and **Supplementary Figure 12A**). Because cells of the TME are thought to be an abundant source of CXCL12 in the MM-TME,[20, 21] we examined the specific contribution of MM-derived CXCL12 by silencing *CXCL12* in *NOTCH3*^{OE} MM cells (**Supplementary Figure 12B**). As seen with Plerixafor, genetic inhibition of *CXCL12* in MM cells restored the anti-MM efficacy of BOR and VRd to control levels (**Figure 6E** and **Supplementary Figure 12C**). These data identify the

existence of a novel autocrine NOTCH3-CXCL12-CXCR4 signaling axis promoted by the TME in MM cells.

Pharmacological inhibition of CXCL12-CXCR4 or Notch signaling increases BOR sensitivity in high NOTCH3 MM cells. Prompted by our *in vitro* studies with Plerixafor, we explored further the use of this agent in combination with BOR-based therapies using MM *ex vivo* 3D organ cultures established with murine and human bone. As seen *in vivo* with BOR, VRd's anti-MM efficacy was significantly reduced in murine bones bearing *NOTCH3*^{OE} vs. control MM cells (**Figure 7A-B**). Co-administration of Plerixafor increased the sensitivity of *NOTCH3*^{OE} MM cells to VRd. We also tested the effects of VRd + Plerixafor in a novel human MM-human bone *ex vivo* system, which allowed us to study MM cell responses to chemotherapy in a TME closer to the one in patients (**Figure 7C**). MM cells engrafted human bones, and tumor growth was evident after four days (**Figure 7C**). *NOTCH3*^{OE} MM cells exhibited resistance to VRd therapy compared to control MM cells, and co-administration of Plerixafor restored VRd's anti-MM efficacy to control levels (**Figure 7D**). Lastly, we investigated if bone-targeted pan inhibition of Notch signals with a novel compound recently developed by our laboratory (BT-GSI)[13] overcomes the chemoresistance conferred by NOTCH3 activation in MM cells. Using *ex vivo* cultures established with murine bone and *Notch3*^{OE} MM cells, we found that co-administration of BT-GSI doubled the anti-MM efficacy of BOR (**Figure 7E-F**). Together, these studies highlight the potential of combining BOR-based therapies with CXCL12-CXCR4 or bone-targeted Notch inhibitors to overcome TME-mediated drug resistance.

Discussion

Chemotherapy resistance is the leading cause of relapsed/refractory disease, decreased survival, and a major obstacle to more successful clinical outcomes in MM. In this study, we demonstrate that a signaling pathway involving NOTCH3 activation by the extrinsic TME in MM cells promotes resistance to BOR therapeutic regimes. Our data highlight that this pathway is present in NDMM patients, upregulated in PRMM patients, and predicts worse clinical responses to BOR-based chemotherapy. Further, genetic activation of NOTCH3 in MM cells is sufficient to promote resistance to BOR therapies. Conversely, we show that genetic or pharmacologic interruption of NOTCH3 signals in MM cells increases sensitivity to BOR and decreases tumor burden. Our clinical and preclinical data position NOTCH3 inhibition as a rational target to improve clinical responses to first-line regimes based on BOR in MM patients.

Osteocytes are best known for their role in bone remodeling, where they function as paracrine and endocrine cells controlling the activity of bone cells in the bone marrow and distant organs.[10] Work from our group and others uncovered that osteocytes are also important components of the TME, capable of directly interacting with tumor cells, and have a pivotal role in tumor growth and cancer-induced bone disease.[22-24] Yet, the role of osteocytes in chemoresistance has not been explored until now. Our studies extend beyond previous work on stromal cell-mediated mechanisms of resistance[3, 4, 8] and identify the osteocyte as a new cell type of the TME contributing to resistance to chemotherapy via Notch communication. Along the same lines, another recent study reported that osteocytes can confer MM resistance to chemotherapy via exosomes.[25] Because osteocytes are 95% of the cells in bone and, as stromal cells, can live for decades, these two cell types represent a major and long-lasting source of pro-survival signals for MM cells in MM. Future studies are needed to characterize further the contextual microenvironments and disease stages where these cell types preferentially operate.

It has been long appreciated that Notch signaling mediates communication between MM cells and other cells of the TME, supports tumor growth and bone destruction, and contributes to drug resistance and survival;[5, 26] furthermore, functional studies have suggested that inhibiting Notch activation downstream all NOTCH receptors with gamma-secretase inhibitors (GSI) decreases tumor burden, bone disease, and improves sensitivity to chemotherapeutic agents.[6, 27] Although the evidence for the influence of NOTCH signals in MM progression is strong, the specific contribution of individual NOTCH components is less clear. Notably, our paper uncovers that the basal expression of *NOTCH3* is dynamic and selectively upregulated by TME cells and describes a previously unknown role for NOTCH3 in MM chemoresistance. Previous *in vitro* studies suggested that NOTCH1 and 2 are the main mediators of stroma-MM communication.[28, 29] In contrast, our prior work showed that osteocytes preferentially employ NOTCH3 to communicate with MM cells.[9] Although we cannot exclude the contribution of other NOTCH receptors to TME-mediated chemoresistance, this study suggests that NOTCH3 activation is a common molecular mechanism that TME cells utilize to communicate with MM cells and plays a pivotal role in promoting drug resistance. We reported before that homotypic NOTCH3 signaling mediates MM cell proliferation but does not affect MM cell viability.[9] Consistent with this observation, homotypic NOTCH3 signaling (between MM cells) did not affect MM cell apoptotic responses to BOR or VRd, underlining their dependence on TME-derived Notch ligands for chemoprotection. Further studies beyond the scope of the current manuscript are granted to identify the TME Notch ligand(s) responsible for the activation of NOTCH3 and chemoresistance in MM cells.

We noted fascinating differences in the transcriptome of NDMM that are mechanistically dependent on NOTCH3 and lead to a gene signature predictive of poor clinical outcomes. Our

data show that NOTCH3 integrates signals from cells of the TME to increase CXCL12 expression in MM cells and provide evidence of NOTCH3-CXCL12 co-expression in $CD138^{+}$ plasma cells from patients. Previous *in vitro* observations showed that inhibition of all NOTCH receptors with GSI decreases CXCL12 production in MM cells.[30] Our findings are consistent with this study and support that NOTCH3 is a major molecular regulator of CXCL12. Although stroma-derived CXCL12/CXCR4 is a well-established symbiotic bridge linking MM cells and their stromal neighbors in oncogenic communication/drug resistance,[8, 17, 18, 20, 21, 31, 32] this report is one of the first indications suggesting the existence of an active autocrine CXCL12-CXCR4 signaling axis in MM cells promoted by the TME. We show that interruption of NOTCH3 signals by inhibiting NOTCH3 cleavage at the membrane level (BT-GSI) or suppressing CXCL12 expression (siRNA) or signaling through CXCR4 (Plerixafor) led to comparable prevention of TME-induced BOR resistance in MM cells. Remarkably, we validated these observations in human *ex vivo* models, which showed that bones infiltrated with NOTCH3-activated MM cells have worse responses to VRd and, importantly, a robust reduction in tumor burden after co-administration of VRd and Plerixafor. Therefore, human (and murine) *ex vivo* organ cultures represent a powerful tool to model responses to chemotherapy in a physiologically relevant environment. Collectively, these findings support that NOTCH3 is activated in MM cells by the TME in specialized niches, resulting in a transcriptional response downstream of CXCL12 binding to CXCR4, which leads to chemoresistance.

In addition to its role in drug resistance, we confirmed that NOTCH3 signaling in MM cells exerts bone catabolic actions. We showed before that inhibition of NOTCH3 in MM cells reduces MM-induced bone disease.[9] Conversely, we found that mice-bearing MM cells with activated NOTCH3 exhibited worse bone destruction in this study. Two potential mechanisms,

not mutually exclusive, may account for this observation. One, NOTCH3 activation by TME cells increases in MM cells the expression of RANKL, a pro-osteoclastogenic cytokine with a key role in the development of bone disease in MM patients.[33, 34] Second, TME-derived signals integrated by NOTCH3 stimulate the proliferation of MM cells and lead to greater tumors and, therefore, more bone disease. Our studies did not address the contribution of each potential mechanism, as both occur simultaneously in our model.

These findings have important clinical implications. Our results suggest the potential added value of NOTCH3 expression in MM treatment decision-making for NDMM and PRMM patients. Further validation of the impact of NOTCH3 expression in other cohorts is needed to strengthen this argument, which we acknowledge as a limitation of our study. In addition, these findings raise the possibility that NOTCH3 might be a useful target for MM patients. Anti-*NOTCH3*-antibodies have shown efficacy against solid tumors[35-37] but have not yet been evaluated in MM models. Further, our data suggest the potential of a therapy targeting NOTCH3 to simultaneously decrease tumor growth, improve responses to BOR regimes, and stop bone destruction, as pharmacological inhibition of *NOTCH3 in vivo* is sufficient to decrease bone resorption in naïve mice.[37] Of note, *NOTCH3*-antibodies do not exhibit dose-limiting side effects[37] seen with pan-inhibition of Notch signaling in humans and mice.[13, 38] Similarly, our novel bone-targeted GSI inhibitor shows great potential to overcome drug resistance mediated by NOTCH3, and other NOTCH receptors, while circumventing toxicities. Lastly, our work provides a cellular and molecular rationale to combine BOR regimes with Plerixafor as a chemosensitization strategy in MM patients, a strategy proven successful recently in a small clinical trial (NCT00903968).[39]

A better understanding of the cellular and molecular events leading to disease progression/relapse in MM is needed to bypass drug resistance. This study unravels a crucial role of NOTCH3 as a mediator of TME-mediated chemoresistance in MM. Complementary clinical and preclinical data and pharmacologic and genetic approaches in human and mouse systems support this conclusion. Further, we identified a previously unknown function of osteocytes as providers of Notch signals in the TME conducive to resistance to chemotherapy. Lastly, we demonstrate the beneficial effects of targeting NOTCH3 and its downstream signals to restore sensitivity to BOR-based therapies in MM cells. In summary, our findings support using existing and novel pharmacologic tools to interfere with NOTCH3 signals to overcome drug resistance and improve bone health in MM.

References

1. Rajkumar SV, Kumar S. Multiple myeloma current treatment algorithms. Blood Cancer J. 2020;10(9):94.
2. Maiso P, Mogollón P, Ocio EM, Garayoa M. Bone Marrow Mesenchymal Stromal Cells in Multiple Myeloma: Their Role as Active Contributors to Myeloma Progression. Cancers (Basel). 2021;13(11):2542.
3. Ria R, Vacca A. Bone Marrow Stromal Cells-Induced Drug Resistance in Multiple Myeloma. Int J Mol Sci. 2020;21(2):613.
4. Nefedova Y, Landowski TH, Dalton WS. Bone marrow stromal-derived soluble factors and direct cell contact contribute to de novo drug resistance of myeloma cells by distinct mechanisms. Leukemia. 2003;17(6):1175-1182.
5. Colombo M, Galletti S, Garavelli S, et al. Notch signaling deregulation in multiple myeloma: A rational molecular target. Oncotarget. 2015;6(29):26826-26840.
6. Nefedova Y, Sullivan DM, Bolick SC, Dalton WS, Gabrilovich DI. Inhibition of Notch signaling induces apoptosis of myeloma cells and enhances sensitivity to chemotherapy. Blood. 2008;111(4):2220-2229.
7. Wang Z, Li Y, Ahmad A, et al. Targeting Notch signaling pathway to overcome drug resistance for cancer therapy. Biochim Biophys Acta. 2010;1806(2):258-267.
8. Colombo M, Garavelli S, Mazzola M, et al. Multiple myeloma exploits Jagged1 and Jagged2 to promote intrinsic and bone marrow-dependent drug resistance. Haematologica. 2020;105(7):1925-1936.

9. Sabol HM, Amorim T, Ashby C, et al. Notch3 signaling between myeloma cells and osteocytes in the tumor niche promotes tumor growth and bone destruction. Neoplasia. 2022;28:100785.
10. Delgado-Calle J, Bellido T. The osteocyte as a signaling cell. Physiol Rev. 2022;102(1):379-410.
11. Choudhury SR, Ashby C, Tytarenko R, et al. The functional epigenetic landscape of aberrant gene expression in molecular subgroups of newly diagnosed multiple myeloma. J Hematol Oncol. 2020;13(1):108.
12. Delgado-Calle J, Anderson J, Cregor MD, et al. Bidirectional Notch Signaling and Osteocyte-Derived Factors in the Bone Marrow Microenvironment Promote Tumor Cell Proliferation and Bone Destruction in Multiple Myeloma. Cancer Res. 2016;76(5):1089-1100.
13. Sabol HM, Ferrari AJ, Adhikari M, et al. Targeting Notch Inhibitors to the Myeloma Bone Marrow Niche Decreases Tumor Growth and Bone Destruction without Gut Toxicity. Cancer Res. 2021;81(19):5102-5114.
14. Delgado-Calle J, Anderson J, Cregor MD, et al. Genetic deletion of Sost or pharmacological inhibition of sclerostin prevent multiple myeloma-induced bone disease without affecting tumor growth. Leukemia. 2017;31(12):2686-2694.
15. Mulligan G, Mitsiades C, Bryant B, et al. Gene expression profiling and correlation with outcome in clinical trials of the proteasome inhibitor bortezomib. Blood. 2007;109(8):3177-3188.
16. Bellido T, Delgado-Calle J. Ex Vivo Organ Cultures as Models to Study Bone Biology. JBMR Plus. 2020;4(3):10.

17. Waldschmidt JM, Simon A, Wider D, et al. CXCL12 and CXCR7 are relevant targets to reverse cell adhesion-mediated drug resistance in multiple myeloma. Br J Haematol. 2017;179(1):36-49.
18. Bouyssou JM, Ghobrial IM, Roccaro AM. Targeting SDF-1 in multiple myeloma tumor microenvironment. Cancer Lett. 2016;380(1):315-318.
19. Cohen YC, Zada M, Wang SY, et al. Identification of resistance pathways and therapeutic targets in relapsed multiple myeloma patients through single-cell sequencing. Nat Med. 2021;27(3):491-503.
20. Ullah TR. The role of CXCR4 in multiple myeloma: Cells' journey from bone marrow to beyond. J Bone Oncol. 2019;17:100253.
21. Ren Z, Lantermans H, Kuil A, et al. The CXCL12gamma chemokine immobilized by heparan sulfate on stromal niche cells controls adhesion and mediates drug resistance in multiple myeloma. J Hematol Oncol. 2021;14(1):11.
22. Anloague A, Delgado-Calle J. Osteocytes: New Kids on the Block for Cancer in Bone Therapy. Cancers (Basel). 2023;15(9):2645.
23. Atkinson EG, Delgado-Calle J. The Emerging Role of Osteocytes in Cancer in Bone. JBMR Plus. 2019;3(3):e10186.
24. Pin F, Prideaux M, Bonewald LF, Bonetto A. Osteocytes and Cancer. Curr Osteoporos Rep. 2021;19(6):616-625.
25. Cheng F, Wang Z, You G, Liu Y, He J, Yang J. Osteocyte-derived exosomes confer multiple myeloma resistance to chemotherapy through acquisition of cancer stem cell-like features. Leukemia. 2023;37(6):1392-1396.

26. Fairfield H, Falank C, Avery L, Reagan MR. Multiple myeloma in the marrow: pathogenesis and treatments. Ann N Y Acad Sci. 2016;1364(1):32-51.
27. Colombo M, Platonova N, Giannandrea D, Palano MT, Basile A, Chiaramonte R. Re-establishing Apoptosis Competence in Bone Associated Cancers via Communicative Reprogramming Induced Through Notch Signaling Inhibition. Front Pharmacol. 2019;10:145.
28. Nefedova Y, Cheng P, Alsina M, Dalton WS, Gabrilovich DI. Involvement of Notch-1 signaling in bone marrow stroma-mediated de novo drug resistance of myeloma and other malignant lymphoid cell lines. Blood. 2004;103(9):3503-3510.
29. Muguruma Y, Yahata T, Warita T, et al. Jagged1-induced Notch activation contributes to the acquisition of bortezomib resistance in myeloma cells. Blood Cancer J. 2017;7(12):650.
30. Mirandola L, Apicella L, Colombo M, et al. Anti-Notch treatment prevents multiple myeloma cells localization to the bone marrow via the chemokine system CXCR4/SDF-1. Leukemia. 2013;27(7):1558-1566.
31. Di Marzo L, Desantis V, Solimando AG, et al. Microenvironment drug resistance in multiple myeloma: emerging new players. Oncotarget. 2016;7(37):60698-60711.
32. Azab AK, Runnels JM, Pitsillides C, et al. CXCR4 inhibitor AMD3100 disrupts the interaction of multiple myeloma cells with the bone marrow microenvironment and enhances their sensitivity to therapy. Blood. 2009;113(18):4341-4351.
33. Raje N, Terpos E, Willenbacher W, et al. Denosumab versus zoledronic acid in bone disease treatment of newly diagnosed multiple myeloma: an international, double-blind, double-dummy, randomised, controlled, phase 3 study. Lancet Oncol. 2018;19(3):370-381.

34. Silbermann R, Roodman GD. Myeloma bone disease: Pathophysiology and management. J Bone Oncol. 2013;2(2):59-69.
35. Varga J, Nicolas A, Petrocelli V, et al. AKT-dependent NOTCH3 activation drives tumor progression in a model of mesenchymal colorectal cancer. J Exp Med. 2020;217(10):e201921515.
36. Choy L, Hagenbeek TJ, Solon M, et al. Constitutive NOTCH3 Signaling Promotes the Growth of Basal Breast Cancers. Cancer Res. 2017;77(6):1439-1452.
37. Yu J, Siebel CW, Schilling L, Canalis E. An antibody to Notch3 reverses the skeletal phenotype of lateral meningocele syndrome in male mice. J Cell Physiol. 2020;235(1):210-220.
38. Golde TE, Koo EH, Felsenstein KM, Osborne BA, Miele L. γ-Secretase inhibitors and modulators. Biochim Biophys Acta. 2013;1828(12):2898-2907.
39. Ghobrial IM, Liu CJ, Zavidij O, et al. Phase I/II trial of the CXCR4 inhibitor plerixafor in combination with bortezomib as a chemosensitization strategy in relapsed/refractory multiple myeloma. Am J Hematol. 2019;94(11):1244-1253.

Figure legends

Figure 1. *NOTCH3* expression is increased in newly diagnosed MM (NDMM) patients and regulated by the cells of the tumor niche. (A) Gene expression of *NOTCH 1-4* receptors in $CD138^+$ cells from NDMM or healthy donors. N=52 patients. *$p<0.05$ vs. healthy donors by One-way ANOVA, followed by a Tukey post hoc test. Boxes show the data interquartile range, the middle line in the box represents the median, and whiskers the 95% confidence interval of the mean. (B) *NOTCH3* gene expression in $CD138^+$ cells from NDMM patients with or without point mutations in the *NOTCH3* gene. N=725 (12 with mutations) NDMM patients.

Figure 2. *NOTCH3* expression is increased in relapsed MM patients and correlates with poor responses to BOR-based therapies. Network plot of selected upregulated functional enrichment analysis of GO terms related to (A) Responses to *Drugs* or (B) *Cell-Adhesion* in $CD138^+$ cells from newly diagnosed (NDMM) patients with high vs. low *NOTCH3* expression. The size of the circles represents the number of genes in the individual GO terms. The thickness of the lines represents the number of overlapped genes between the individual GO terms. (C) Gene Set Enrichment Analysis (GSEA) shows NDMM patients with high *NOTCH3* have enrichment in genes involved in poor responses to Bortezomib (BOR) therapy in MM patients compared to NDMM patients with low *NOTCH3* expression. Data were analyzed using a weighted Kolmogorov-Smirnov-like statistical test. (D) Kaplan-Meier plot of the progression-free survival (PFS) of NDMM patients with high (top) vs. low (bottom) *NOTCH3* expression receiving BOR-based (blue line) vs. other therapies (other) not including BOR (red line). N=708 patients. Data were analyzed using a Log-rank (Mantel-Cox) test. (E) Gene expression of *NOTCH 1-4* receptors in $CD138^+$ cells from paired diagnosis (NDMM) and progression/relapsed MM (PRMM) patients. N=70/group. *$p<0.05$ vs. diagnosis by Student's *t*-test. Boxes show the

data interquartile range, the middle line in the box represents the median, and whiskers the 95% confidence interval of the mean.

Figure 3. NOTCH3 integrates TME-mediated signals dictating MM cell responses to BOR-based therapies. (A) MM cells were co-cultured with osteocytes (Ots) and treated with Bortezomib (BOR; 48h) or Dexamethasone+BOR+Lenalidomide (VRd; 24h). Percent apoptosis in scramble (Scr) or *NOTCH3* knockdown (*NOTCH3*^{KD}) 5TGM1 or U266 (B) MM cells, and in Scr or *NOTCH3* activated (*NOTCH3*^{OE}) OPM2 (C) MM cells co-cultured in the absence/presence of Ots and treated with/without BOR or VRd. N=4/group. *p<0.05 by Two-Way ANOVA, followed by a Tukey post hoc test. The dotted line represents the percent apoptosis in vehicle-treated Scr MM cells cultured alone. ns: non-significant. Data are shown as mean ± SD; each dot represents an independent sample. Representative experiments out of two are shown. DiD: cell label dye; PI: propidium iodide.

Figure 4. NOTCH3 activation in MM cells promotes chemoresistance to BOR therapy. (A) Experimental design. Tumor progression and Bortezomib (BOR)-induced tumor reduction (B) and probability of survival (C) in mice injected with Scramble (Scr) or *NOTCH3* activated (*NOTCH3*^{OE}) OPM2 MM cells treated with/without BOR. N=6/11 mice/group. A Two-way ANOVA test was used for (B, endpoint), followed by a Tukey post hoc test. Tumor reduction by BOR therapy by Student's *t*-test, *p<0.05 vs. mice bearing Scr tumors treated with BOR. For (C), a Log-rank (Mantel-Cox) test was performed. (D) Tumor reduction by BOR in *ex vivo* organ cultures of calvarial disc bones from KaLwRijHsd bearing murine 5TGM1 (E) or NSG mice bearing human U266 (F) Scr/*NOTCH3* knockdown (*NOTCH3*^{KD}) MM cells. N=4-8/group. *p<0.05 vs. Scr MM cells treated with BOR by Student's *t*-test for each time point. ns: non-

significant. wk: week. Boxes show the data interquartile range, the middle line in the box represents the median, and whiskers the 95% confidence interval of the mean. (D, E, F).

Figure 5. Activation of NOTCH3 transcriptional reprogramming by the TME increases *CXCL12* expression in MM cells. Top 20 most significantly upregulated pathways (A) in newly diagnosed (NDMM) patients with high vs. low *NOTCH3* expression. N=768 patients. (B) *CXCL12* and *NOTCH3* expression correlation in $CD138^+$ cells from NDMM and progression/relapsed (PRMM) patients. N=70/group. For (B), Pearson's correlation tests were performed. (C) Gene expression of *CXCL12* in $CD138^+$ cells from paired diagnosis and relapsed MM patients. N=70/group. *p<0.05 vs. diagnosis by Student's t-test. Boxes show the data interquartile range, the middle line in the box represents the median, and whiskers the 95% confidence interval of the mean. *CXCL12* gene expression in Scramble (Scr)/*NOTCH3* knockdown ($NOTCH3^{KD}$) 5TGM1 (D) or U266 (E) MM cells and Scr/*NOTCH3* activated ($NOTCH3^{OE}$) OPM2 (F) MM cells cultured in the absence/presence of osteocytes (Ots). N=4/group. *p<0.05 by Two-way ANOVA, followed by a Tukey post hoc test. ns: non-significant. Data are shown as mean ± SD; each dot represents an independent sample; representative experiments out of two are shown (F).

Figure 6. NOTCH3-CXCL12-CXCR4 signaling mediates TME-induced chemoresistance in MM cells. Effects of osteocytes (Ots) and manipulation of NOTCH3 signaling in MM cells on protein levels of activated NOTCH3 receptor (NICD3), phosphorylated (p) CXCR4, pERK, pAKT in (A) Scramble (Scr)/*NOTCH3* knockdown ($NOTCH3^{KD}$) 5TGM1 MM cells and (B) Scr/*NOTCH3* activated ($NOTCH3^{OE}$) OPM2 MM cells. Representative images from 3 independent experiments are shown (see **Supplementary Figure 11**). (C) Experimental design. (D) Percent apoptosis of OPM2 $NOTCH3^{OE}$ MM cells treated with/without Plerixafor,

Bortezomib (BOR), or dexamethasone+BOR+Lenalidomide (VRd) in the absence/presence of Ots. N=4/group; BOR=48h, VRd=24h. (E) Percent apoptosis of OPM2 *NOTCH3*^{OE} MM cells with/without *CXCL12* silencing and treated with BOR or VRd in the absence/presence of Ots. *p<0.05 by Two-way ANOVA, followed by a Tukey post hoc test. The dotted line represents the percent apoptosis in vehicle-treated OPM2 *NOTCH3*^{OE} MM cells cultured alone. ns: non-significant. DiD: cell label dye. siRNA: small interference RNA. Data are shown as mean ± SD; each dot represents an independent sample; representative experiments out of two are shown.

Figure 7. Pharmacological inhibition of CXCL12-CXCR4 or Notch signaling enhances therapeutic responses to BOR-based therapy in NOTCH3-activated MM cells. (A) *Ex vivo* bone-MM organ cultures established with Scramble (Scr)/ *NOTCH3* activated (*NOTCH3*^{OE}) OPM2 human MM cells and calvarial disc bones from NSG mice. (B) Percent tumor reduction by co-administration of dexamethasone+bortezomib (BOR)+lenalidomide (VRd) and Plerixafor. N=6/group. *p<0.05 vs. bones bearing Scr MM cells treated with VRd alone for 11 days by One-way ANOVA, followed by a Tukey post hoc test. (C) *Ex vivo* bone-MM organ cultures established with Scr/*NOTCH3*^{OE} OPM2 human MM cells and femoral head bone fragments from healthy human donors. Representative bioluminescence images of human bones showing engraftment and growth of human MM cells through the length of the experiment. (D) Percent tumor reduction by co-administration of VRd and Plerixafor. N=6/group. *p<0.05 by Two-way ANOVA, followed by a Tukey post hoc test. (E) *Ex vivo* bone-MM organ cultures established with *NOTCH3*^{OE} OPM2 human MM cells and calvarial disc bones from NSG mice. (F) Percent tumor reduction by co-administration of BOR and bone-targeted gamma-secretase inhibitor (BT-GSI) after 4 and 11 days. N=6/group. *p<0.05 vs. bones bearing *NOTCH3*^{OE} MM cells treated with BOR alone by One-way ANOVA, followed by a Tukey post hoc test. ns: non-significant.

Boxes show the interquartile range, the middle line in the box represents the median, and whiskers the 95% confidence interval of the mean. d: days.

Figure 1

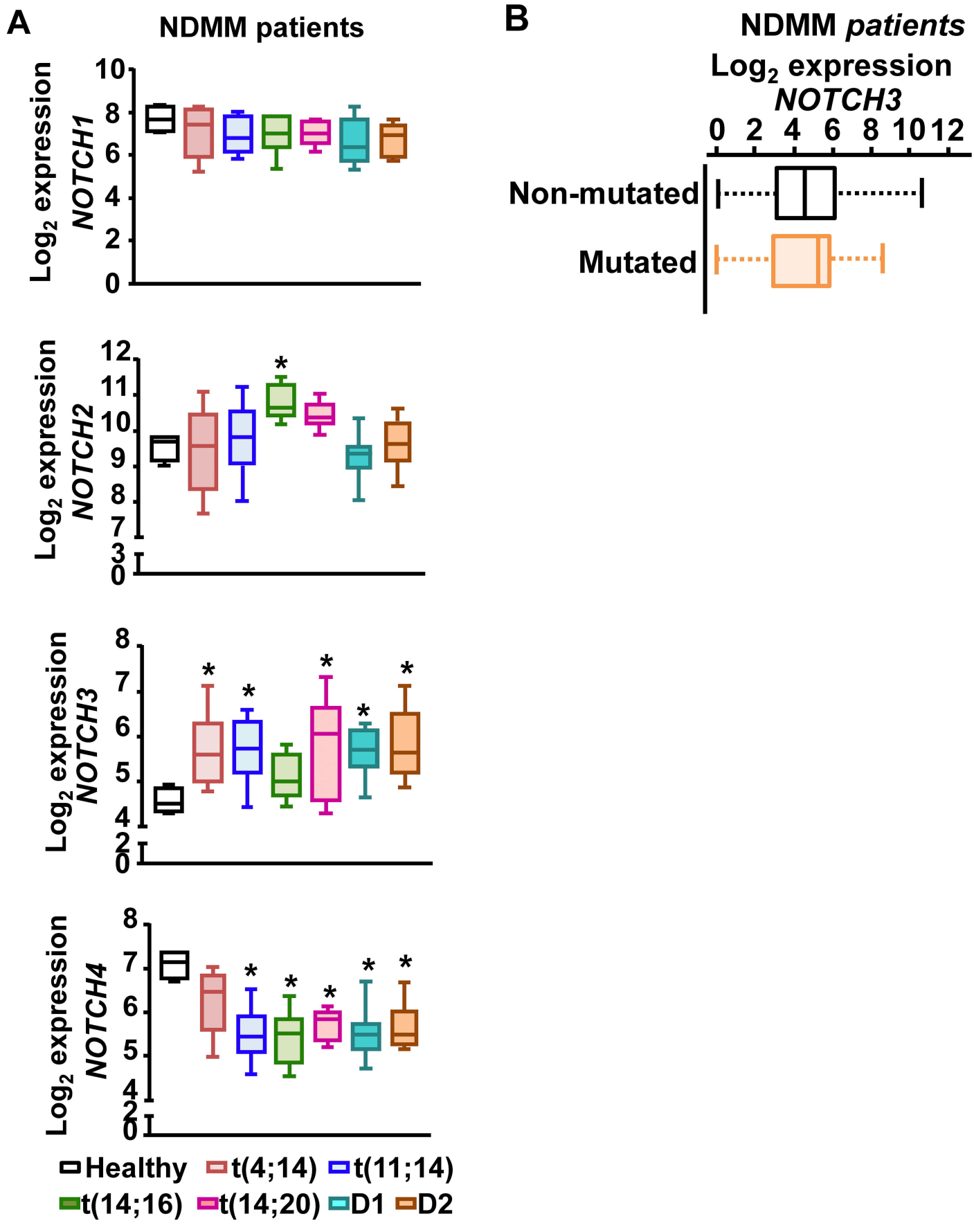
A
NDMM patients
Log2 expression NOTCH1
Log2 expression NOTCH2
Log2 expression NOTCH3
Log2 expression NOTCH4
Healthy
t(4;14)
t(11;14)
t(14;16)
t(14;20)
D1
D2
B
NDMM patients
Log2 expression
NOTCH3
0 2 4 6 8 10 12
Non-mutated
Mutated

Figure 2

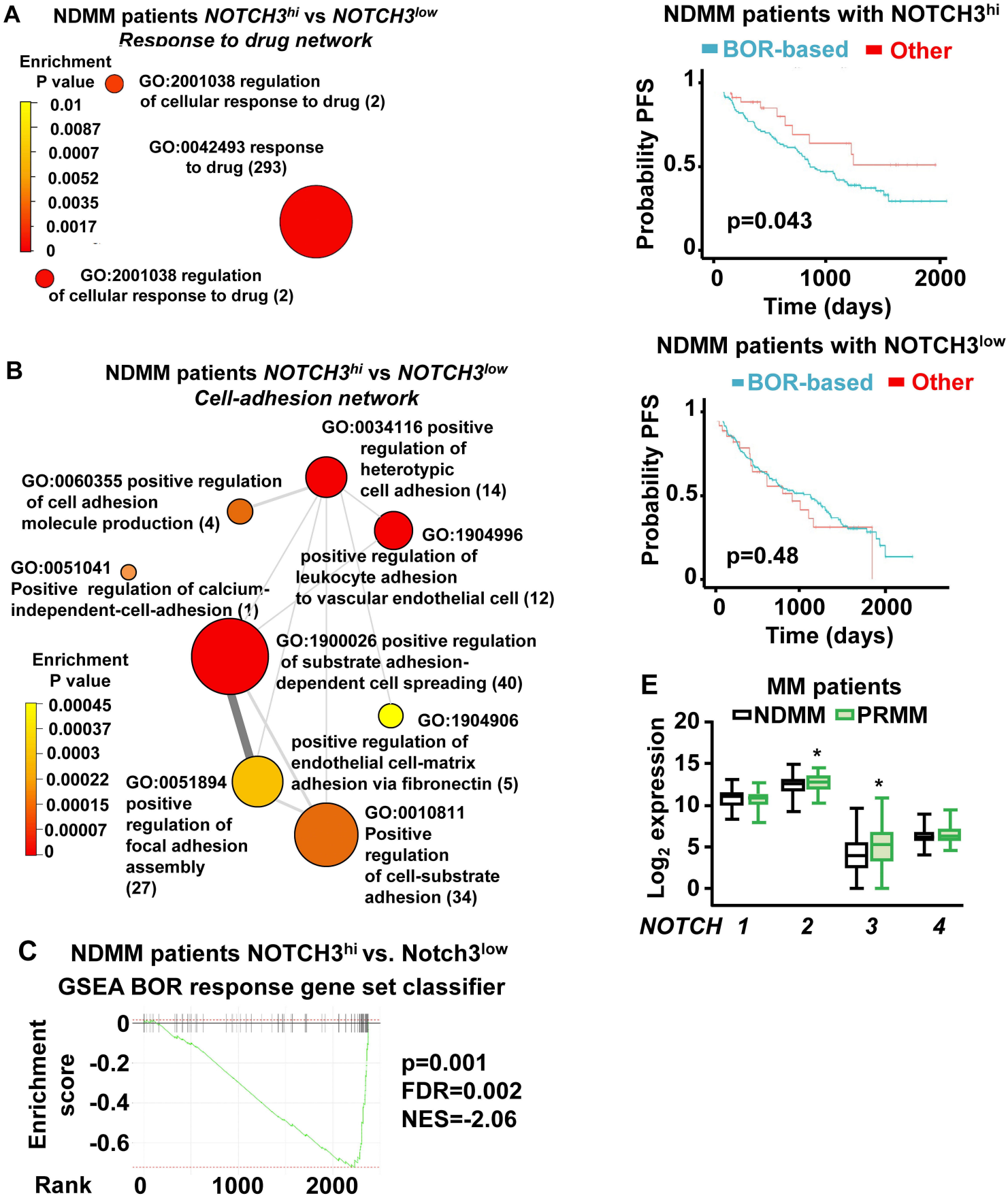
A
NDMM patients NOTCH3hi vs NOTCH3low
Response to drug network
Enrichment
P value
0.01
0.0087
0.0007
0.0052
0.0035
0.0017
0
GO:2001038 regulation of cellular response to drug (2)
GO:0042493 response to drug (293)
GO:2001038 regulation of cellular response to drug (2)
B
NDMM patients NOTCH3hi vs NOTCH3low
Cell-adhesion network
GO:0034116 positive regulation of heterotypic cell adhesion (14)
GO:0060355 positive regulation of cell adhesion molecule production (4)
GO:1904996 positive regulation of leukocyte adhesion to vascular endothelial cell (12)
GO:0051041 Positive regulation of calcium-independent-cell-adhesion (1)
GO:1900026 positive regulation of substrate adhesion-dependent cell spreading (40)
Enrichment
P value
0.00045
0.00037
0.0003
0.00022
0.00015
0.00007
0
GO:1904906 positive regulation of endothelial cell-matrix adhesion via fibronectin (5)
GO:0051894 positive regulation of focal adhesion assembly (27)
GO:0010811 Positive regulation of cell-substrate adhesion (34)
C
NDMM patients NOTCH3hi vs. Notch3low
GSEA BOR response gene set classifier
Enrichment score
0
-0.2
-0.4
-0.6
Rank
0
1000
2000
p=0.001
FDR=0.002
NES=-2.06
D
NDMM patients with NOTCH3hi
BOR-based
Other
Probability PFS
1
0.5
0
p=0.043
0
1000
2000
Time (days)
NDMM patients with NOTCH3low
BOR-based
Other
Probability PFS
1
0.5
0
p=0.48
0
1000
2000
Time (days)
E
MM patients
NDMM
PRMM
Log2 expression
20
15
10
5
0
*
*
NOTCH 1
2
3
4

Figure 3

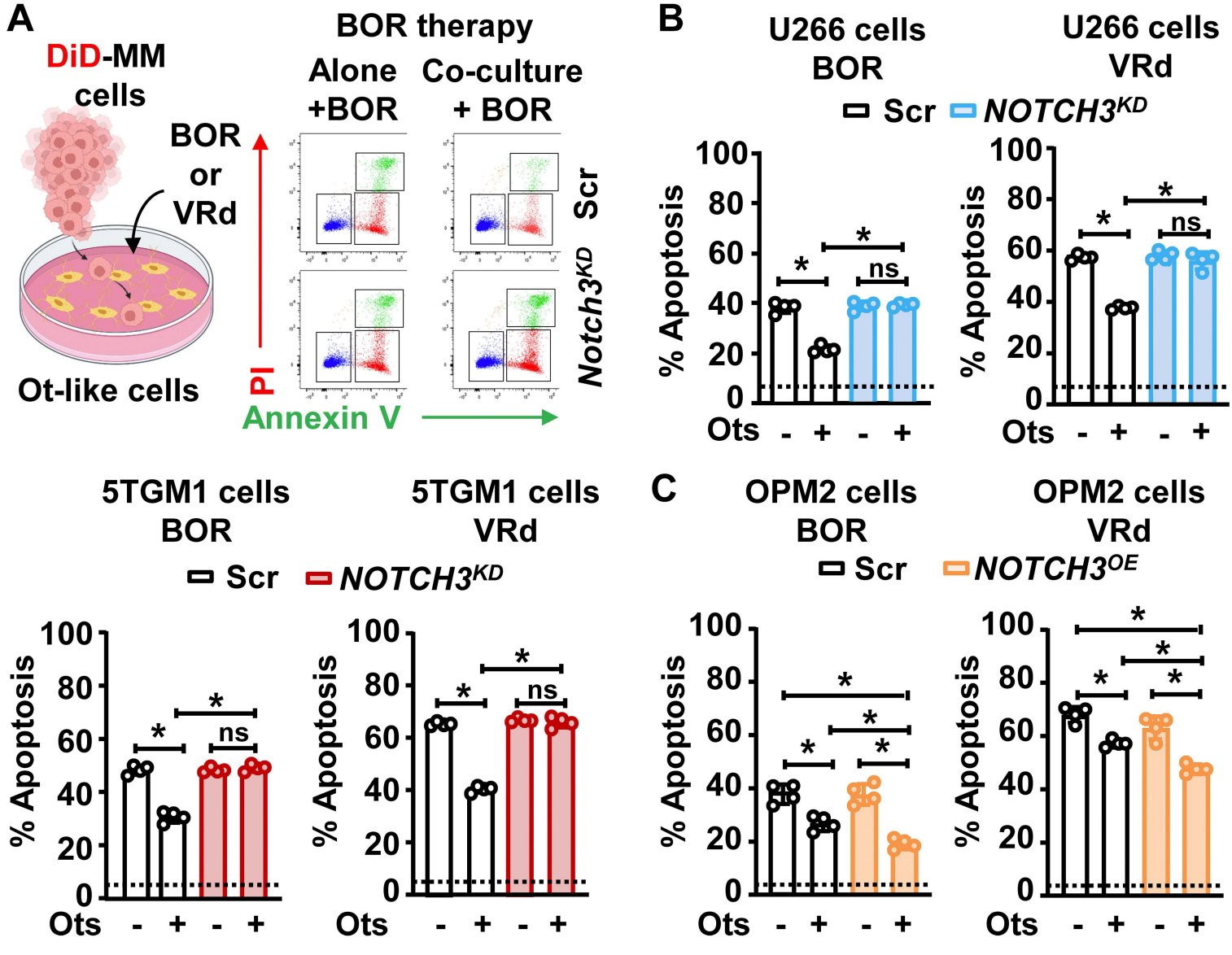
A
DiD-MM cells
BOR or VRd
Ot-like cells
BOR therapy
Alone +BOR
Co-culture + BOR
Scr
Notch3KD
PI
Annexin V
B
U266 cells BOR
U266 cells VRd
Scr
NOTCH3KD
% Apoptosis
Ots
5TGM1 cells BOR
5TGM1 cells VRd
C
OPM2 cells BOR
OPM2 cells VRd
NOTCH3OE
ns

Figure 4

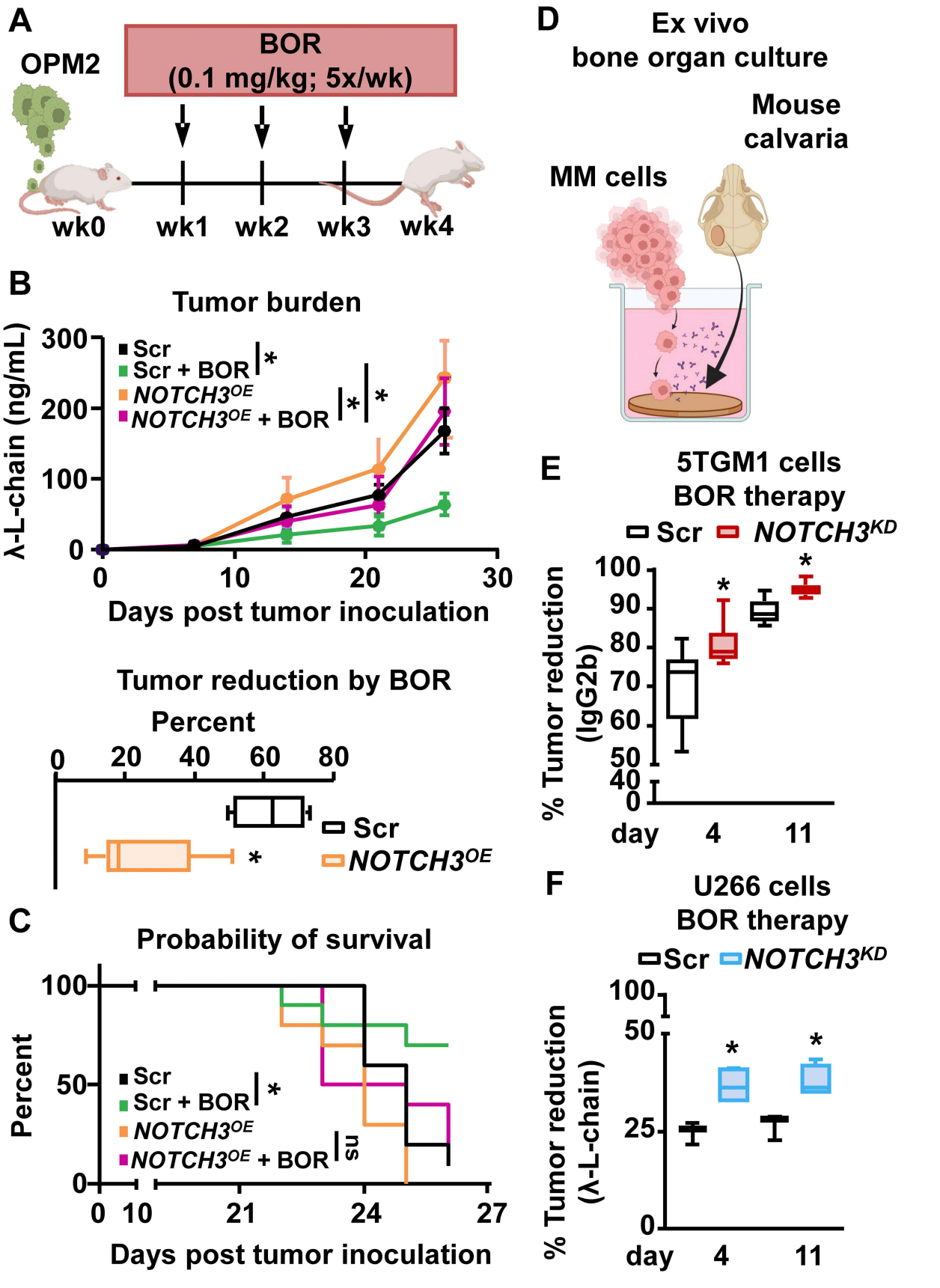
A
OPM2
BOR
(0.1 mg/kg; 5x/wk)
wk0
wk1
wk2
wk3
wk4
B
Tumor burden
λ-L-chain (ng/mL)
Scr
Scr + BOR
NOTCH3OE
NOTCH3OE + BOR
Days post tumor inoculation
Tumor reduction by BOR
Percent
Scr
NOTCH3OE
C
Probability of survival
Percent
Scr
Scr + BOR
NOTCH3OE
NOTCH3OE + BOR
ns
Days post tumor inoculation
D
Ex vivo
bone organ culture
Mouse
calvaria
MM cells
E
5TGM1 cells
BOR therapy
Scr
NOTCH3KD
% Tumor reduction
(IgG2b)
day
F
U266 cells
BOR therapy
Scr
NOTCH3KD
% Tumor reduction
(λ-L-chain)
day

Figure 5

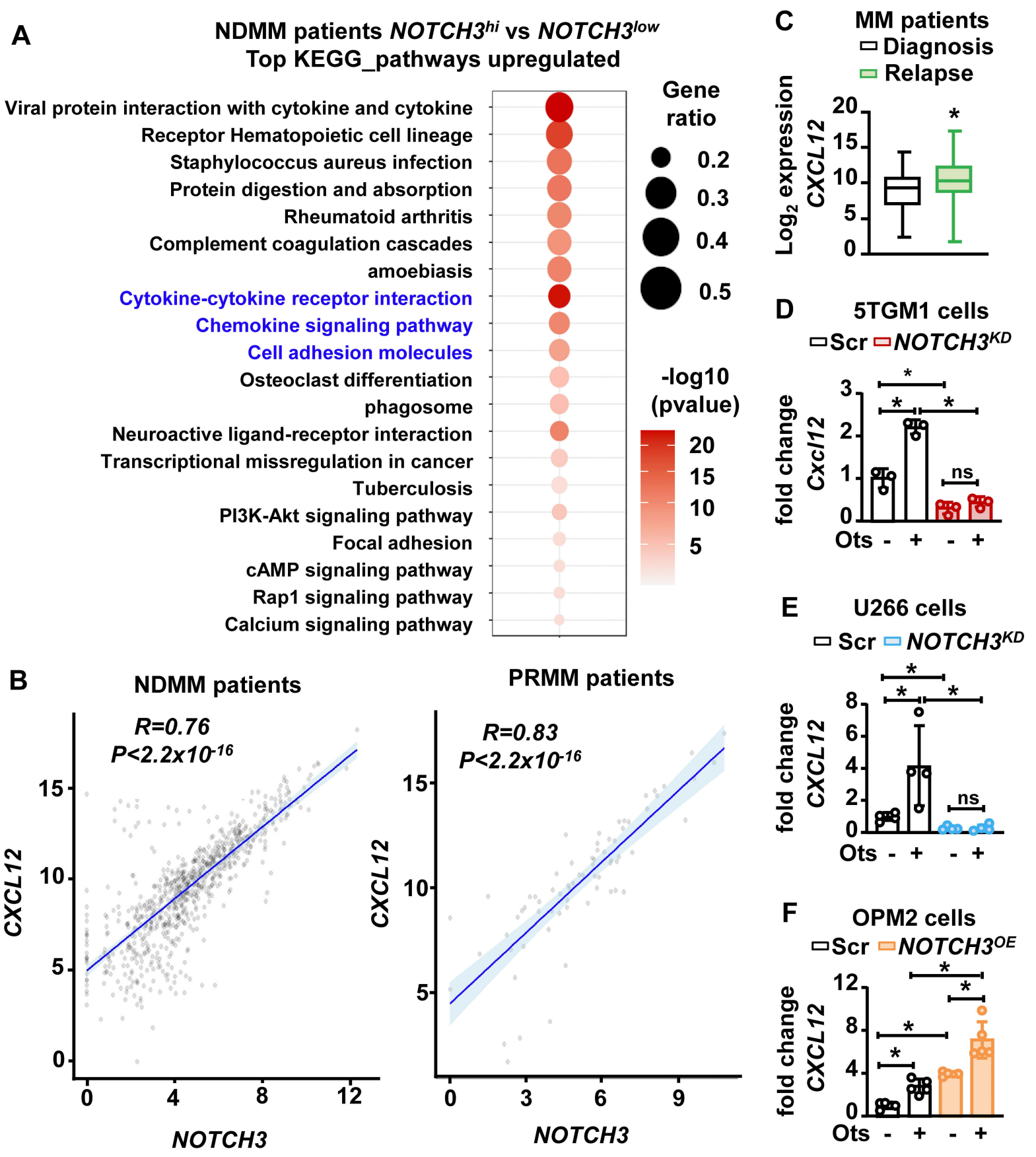
A
NDMM patients NOTCH3hi vs NOTCH3low
Top KEGG_pathways upregulated
Viral protein interaction with cytokine and cytokine
Receptor Hematopoietic cell lineage
Staphylococcus aureus infection
Protein digestion and absorption
Rheumatoid arthritis
Complement coagulation cascades
amoebiasis
Cytokine-cytokine receptor interaction
Chemokine signaling pathway
Cell adhesion molecules
Osteoclast differentiation
phagosome
Neuroactive ligand-receptor interaction
Transcriptional missregulation in cancer
Tuberculosis
PI3K-Akt signaling pathway
Focal adhesion
cAMP signaling pathway
Rap1 signaling pathway
Calcium signaling pathway
Gene ratio
0.2
0.3
0.4
0.5
-log10 (pvalue)
20
15
10
5
B
NDMM patients
R=0.76
P<2.2x10-16
CXCL12
NOTCH3
PRMM patients
R=0.83
P<2.2x10-16
CXCL12
NOTCH3
C
MM patients
Diagnosis
Relapse
Log2 expression CXCL12
D
5TGM1 cells
Scr
NOTCH3KD
fold change Cxcl12
ns
Ots
E
U266 cells
Scr
NOTCH3KD
fold change CXCL12
ns
Ots
F
OPM2 cells
Scr
NOTCH3OE
fold change CXCL12
Ots

Figure 6

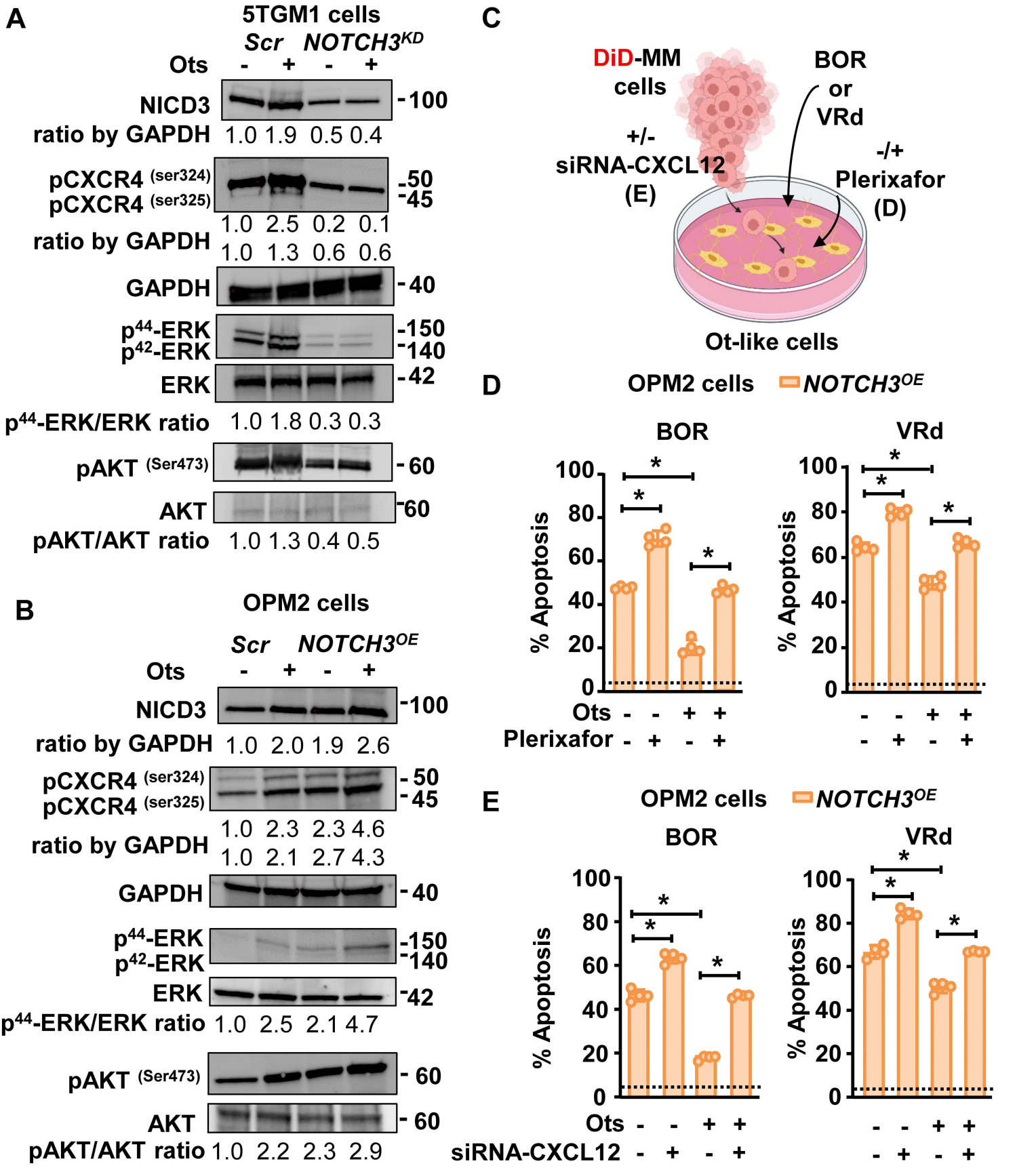
A
5TGM1 cells
Scr
NOTCH3KD
Ots - + - +
NICD3
-100
ratio by GAPDH 1.0 1.9 0.5 0.4
pCXCR4 (ser324)
pCXCR4 (ser325)
-50
-45
1.0 2.5 0.2 0.1
ratio by GAPDH 1.0 1.3 0.6 0.6
GAPDH
-40
p44-ERK
p42-ERK
-150
-140
ERK
-42
p44-ERK/ERK ratio 1.0 1.8 0.3 0.3
pAKT (Ser473)
-60
AKT
-60
pAKT/AKT ratio 1.0 1.3 0.4 0.5
B
OPM2 cells
Scr
NOTCH3OE
Ots - + - +
NICD3
-100
ratio by GAPDH 1.0 2.0 1.9 2.6
pCXCR4 (ser324)
pCXCR4 (ser325)
-50
-45
1.0 2.3 2.3 4.6
ratio by GAPDH 1.0 2.1 2.7 4.3
GAPDH
-40
p44-ERK
p42-ERK
-150
-140
ERK
-42
p44-ERK/ERK ratio 1.0 2.5 2.1 4.7
pAKT (Ser473)
-60
AKT
-60
pAKT/AKT ratio 1.0 2.2 2.3 2.9
C
DiD-MM cells
+/- siRNA-CXCL12 (E)
BOR or VRd
-/+ Plerixafor (D)
Ot-like cells
D
OPM2 cells
NOTCH3OE
BOR
VRd
% Apoptosis
100
80
60
40
20
0
*
Ots - - + +
Plerixafor - + - +
E
OPM2 cells
NOTCH3OE
BOR
VRd
% Apoptosis
Ots - - + +
siRNA-CXCL12 - + - +

Figure 7

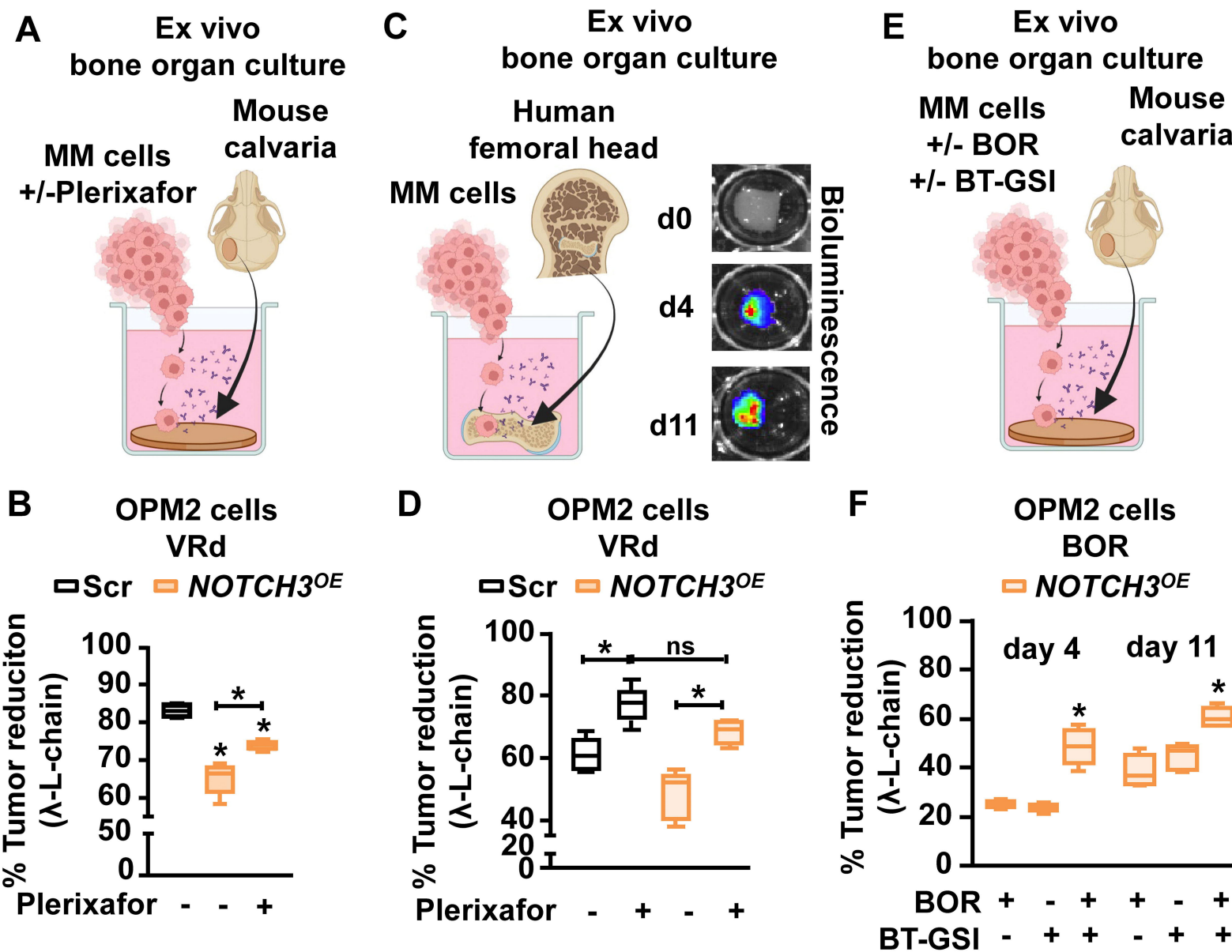
A
Ex vivo
bone organ culture
MM cells
+/-Plerixafor
Mouse
calvaria
C
Ex vivo
bone organ culture
Human
femoral head
MM cells
d0
d4
d11
Bioluminescence
E
Ex vivo
bone organ culture
MM cells
+/- BOR
+/- BT-GSI
Mouse
calvaria
B
OPM2 cells
VRd
Scr
NOTCH3OE
% Tumor reduciton
(λ-L-chain)
100
90
80
70
60
50
0
*
*
*
Plerixafor - - +
D
OPM2 cells
VRd
Scr
NOTCH3OE
% Tumor reduction
(λ-L-chain)
100
80
60
40
20
0
*
ns
*
Plerixafor - + - +
F
OPM2 cells
BOR
NOTCH3OE
% Tumor reduction
(λ-L-chain)
day 4
day 11
100
80
60
40
20
0
*
*
BOR + - + + - +
BT-GSI - + + - + +

Chr	Position	Ref	Alt	Sample
19	15276696	G	A	MMRF_1037_1_BM
19	15299048	G	A	MMRF_1078_1_BM
19	15272330	G	A	MMRF_1290_1_BM
19	15278081	C	T	MMRF_1401_1_BM
19	15303250	C	T	MMRF_1689_1_BM
19	15272059	T	C	MMRF_1755_1_BM
19	15299116	C	G	MMRF_1796_1_BM
19	15281535	G	A	MMRF_1981_1_BM
19	15291836	C	T	MMRF_2314_1_BM
19	15281260	G	A	MMRF_2723_1_BM
19	15284979	G	A	MMRF_2834_1_BM
19	15291067	C	G	MMRF_2843_1_BM

Supplementary Table 1. Point mutations in the *NOTCH3* gene detected in newly diagnosed MM patients from the MMRF. N=725 patients. Chr: chromosome; Ref: reference nucleotide; Atl: alteration.

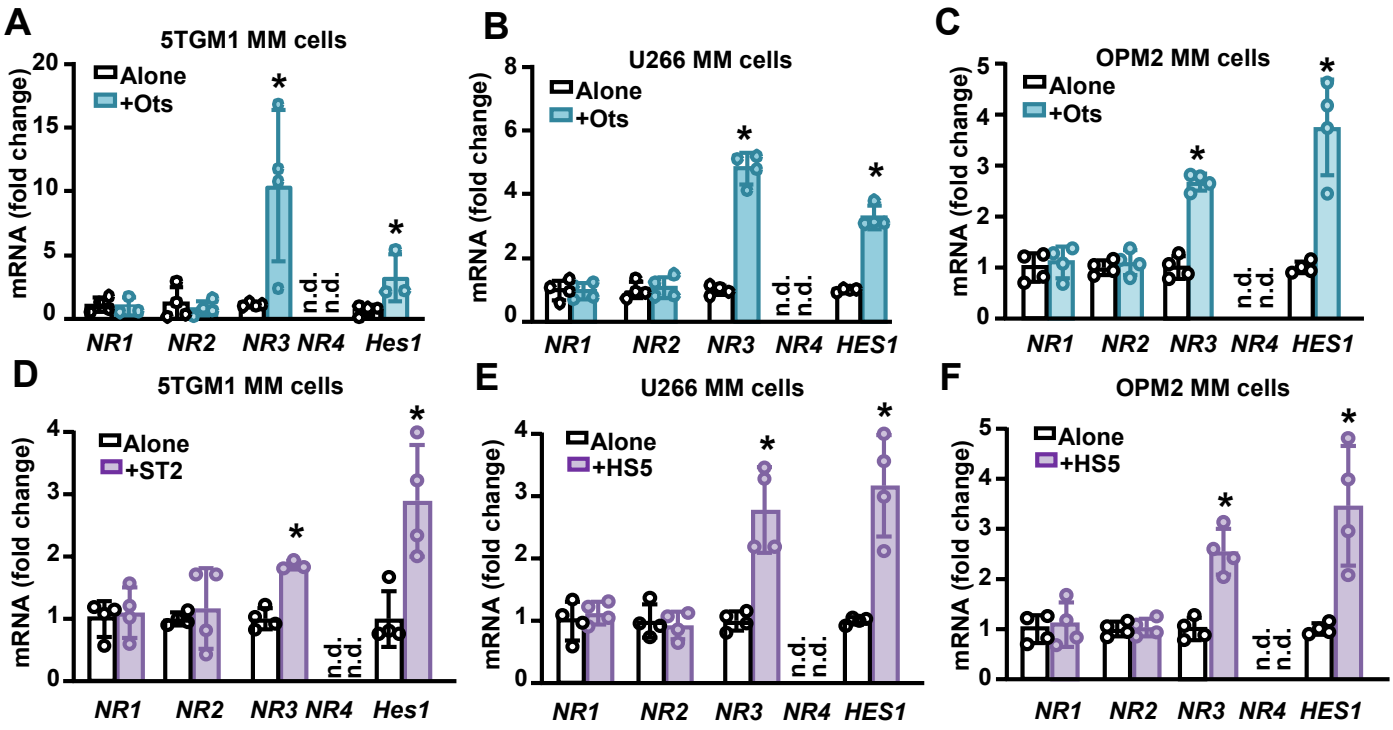

Supplementary Figure 1. Cells of the TME increase *NOTCH3* expression in MM cell lines. Gene expression of NOTCH receptors (*NR*) 1-4 and the Notch target gene *HES1* in co-cultures of osteocytes (Ots) and (A) murine 5TGM1, (B) human U266, or (C) human OPM2 MM cells after 48h. mRNA expression of (D) murine 5TGM1, (E) human U266, and (F) human OPM2 MM cells cultured in the absence and presence of stromal cells (ST2: murine stromal cells; HS-5: human stromal cells). N=4/group. *p<0.05 vs. MM cells cultured alone by Student's *t*-test. n.d.: not detected. Data are shown as mean ± SD; each dot represents an independent sample. Representative experiments out of two are shown.

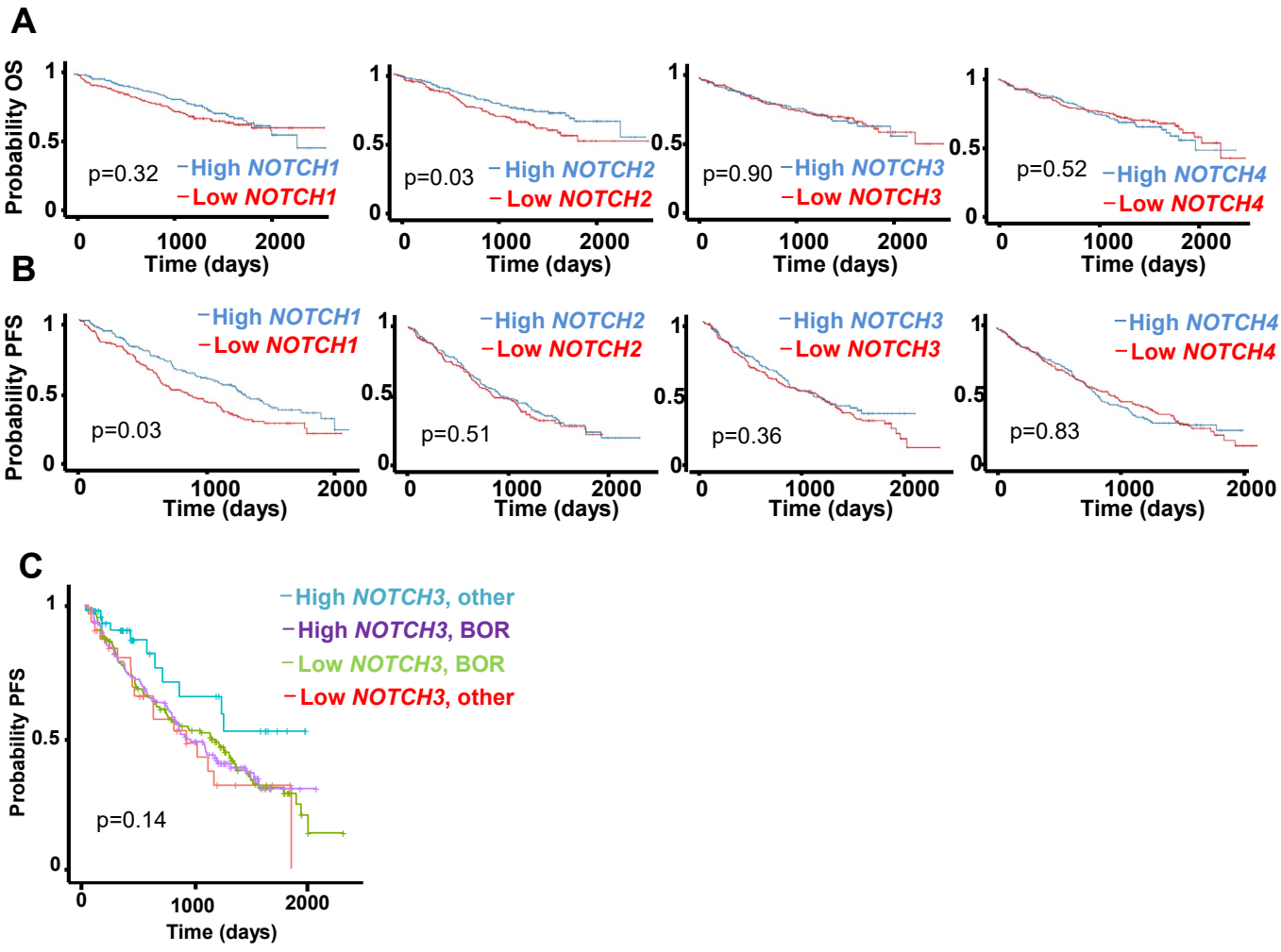

Supplementary Figure 2. Correlation between *NOTCH1-4* expression and survival in newly diagnosed MM patients. Kaplan-Meier plots of the overall survival (OS, A) and progression-free survival (PFS, B) of newly diagnosed MM (NDMM) patients with high (blue) vs. low (red) *NOTCH 1-4* expression. (C) Kaplan-Meier plot of the PFS of NDMM patients with high *NOTCH3* expression receiving Bortezomib (BOR)-based therapy (purple line), high *NOTCH3* expression receiving other therapies not including BOR (other; sky blue line), low *NOTCH3* expression receiving BOR-based therapy (green line), low *NOTCH3* expression receiving other therapies not including BOR (other; red line). N=708 patients. Data were analyzed using a Log-rank (Mantel-Cox) test.

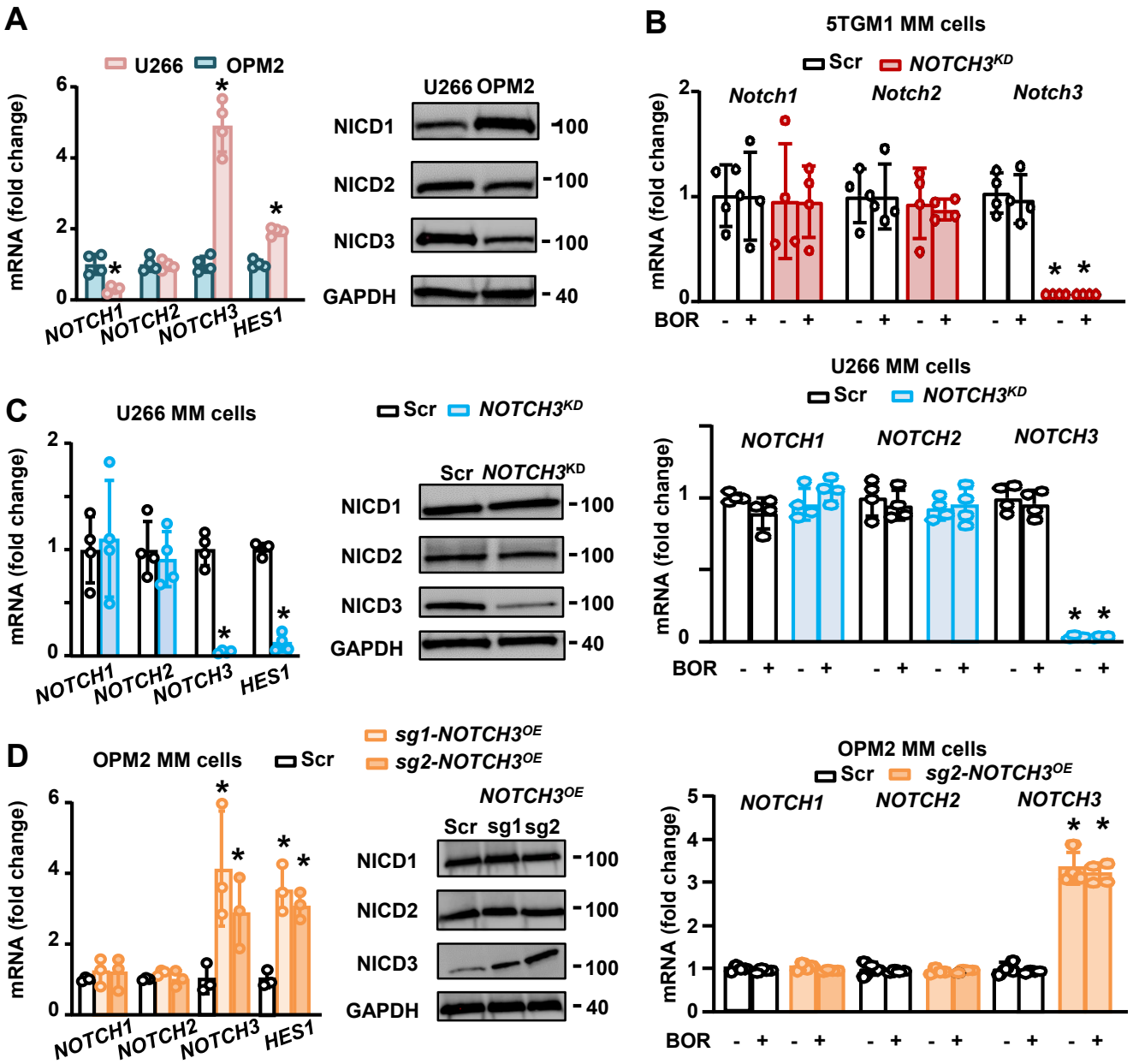

Supplementary Figure 3. Generation of *NOTCH3* knockdown and activated MM cells. (A) *NOTCH1-3* receptor expression and cleaved intracellular domain (NICD) protein levels in human U266 and OPM2 MM cells. N=4/group; 48h culture. *p<0.05 vs OPM2 cells by Student's *t*-test. (B) *NOTCH 1-3* gene expression in scramble (Scr) or genetically modified 5TGM1, U266, and OPM2 MM cells cultured alone and treated with Bortezomib (BOR; 3nM) for 24h. N=4/group; *p<0.05 vs. scramble MM cells by Two-Way ANOVA, followed by a Tukey post hoc test. *NOTCH 1-3* and *HES1* gene expression and cleaved NICD protein levels in (C) U266 Scr and *NOTCH3* knockdown (*NOTCH3*^{KD}) MM cells and (D) OPM2 Scr and *NOTCH3* activated (*NOTCH3*^{OE}) MM cells. N=4/group; 48h culture. *p<0.05 vs. Scr MM cells by Student's *t*-test (C) or One-Way ANOVA, followed by a Tukey post hoc test (D). Data are shown as mean ± SD; each dot represents an independent sample. Representative experiments out of two are shown. sg: guide RNA.

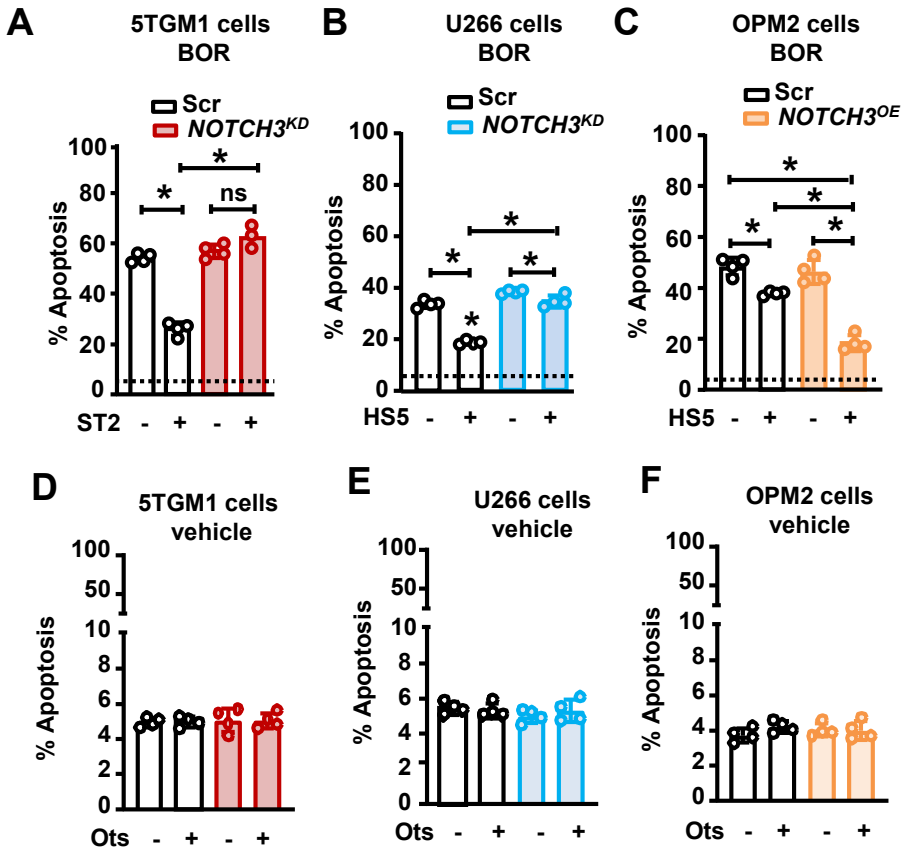

Supplementary Figure 4. NOTCH3 acts as a signaling hub integrating stroma-mediated drug resistance signals. Percent apoptosis in (A) 5TGM1 scramble (Scr)/*NOTCH3* knockdown (*NOTCH3*^{KD}) MM cells, (B) U266 Scr/*NOTCH3*^{KD} MM cells, and (C) OPM2 Scr/*NOTCH3* activated (*NOTCH3*^{OE}) MM cells cultured in the absence/presence of stromal cells treated with Bortezomib (BOR). Percent apoptosis in (D) 5TGM1 Scr/*NOTCH3*^{KD} MM cells, (E) U266 Scr/*NOTCH3*^{KD} MM cells, and (F) OPM2 Scr/*NOTCH3*^{OE} MM cells cultured in the absence/presence of osteocytes cultured without BOR. N=4/group; BOR=48h. *p<0.05 by Two-way ANOVA, followed by a Tukey post hoc test. Ots: osteocyte-like cells; ST2: murine stromal cells; HS-5: human stromal cells. Dotted line represents the percent apoptosis in vehicle-treated Scr MM cells cultured alone. ns: non-significant. Data are shown as mean ± SD; each dot represents an independent sample. Representative experiments out of two are shown.

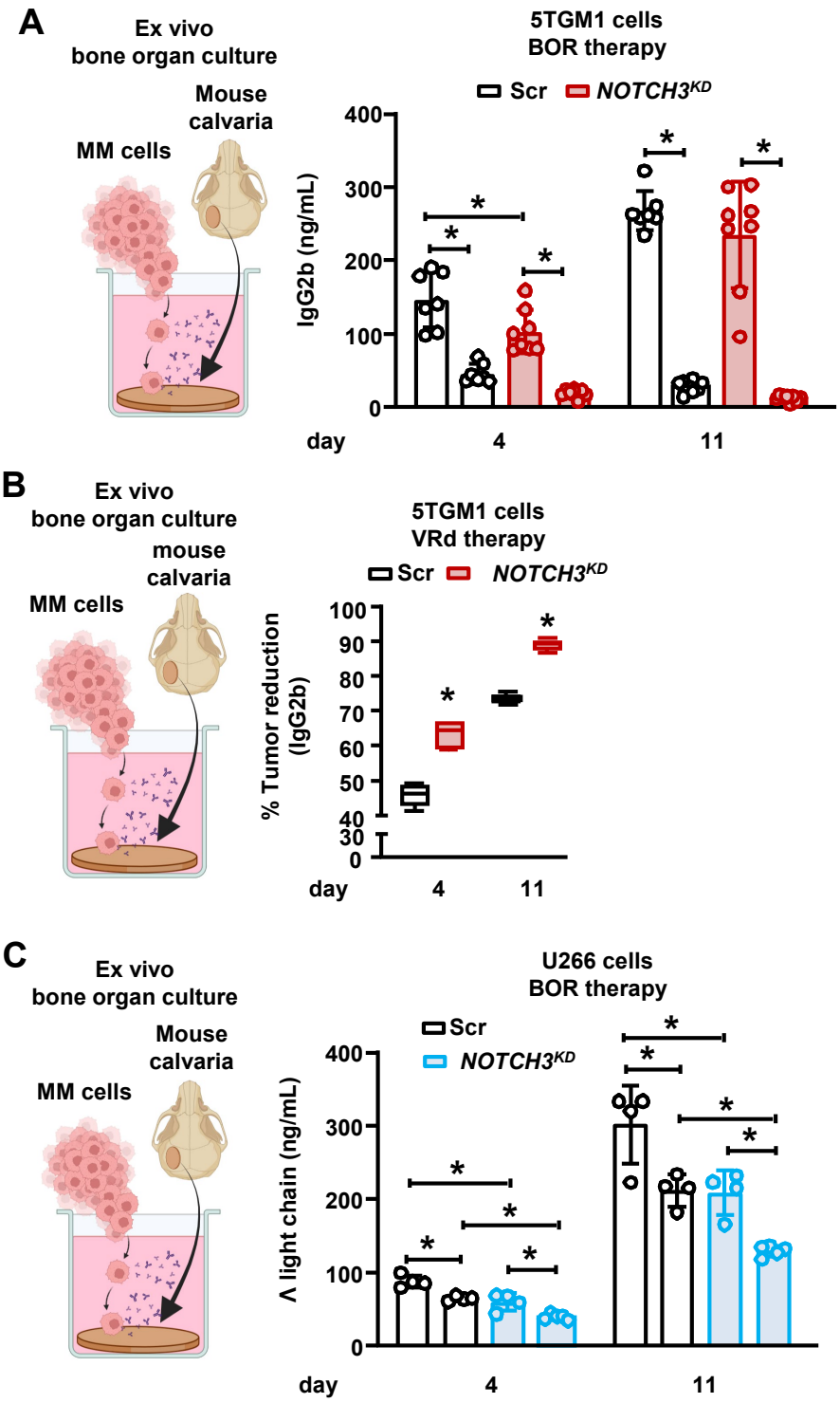

Supplementary Figure 5. Inhibition of *NOTCH3* sensitizes MM cells to Bortezomib-based treatment. *Ex vivo* bone-MM organ cultures were established with murine scramble (Scr) and *NOTCH3* knockdown (*NOTCH3*^{KD}) 5TGM1 MM cells and calvarial disc bones from C57BL/KaLwRijHsd mice (A, B) or human Scr and *NOTCH3*^{KD} U266 MM cells and calvarial disc bones from NSG mice (C). Cultures were treated with Bortezomib (BOR) (A, C) or dexamethsasone+BOR+Lenalidomide (VRd) (B) for 4 and 11 days. N=4-8/group. *p<0.05 by Two-way ANOVA, followed by a Tukey post hoc test (A, C) or Student's *t*-test (B). Data are shown as mean ± SD (A, C); each dot represents an independent sample. Boxes show the data interquartile range, the middle line in the box represents the median, and whiskers the 95% confidence interval of the mean (B).

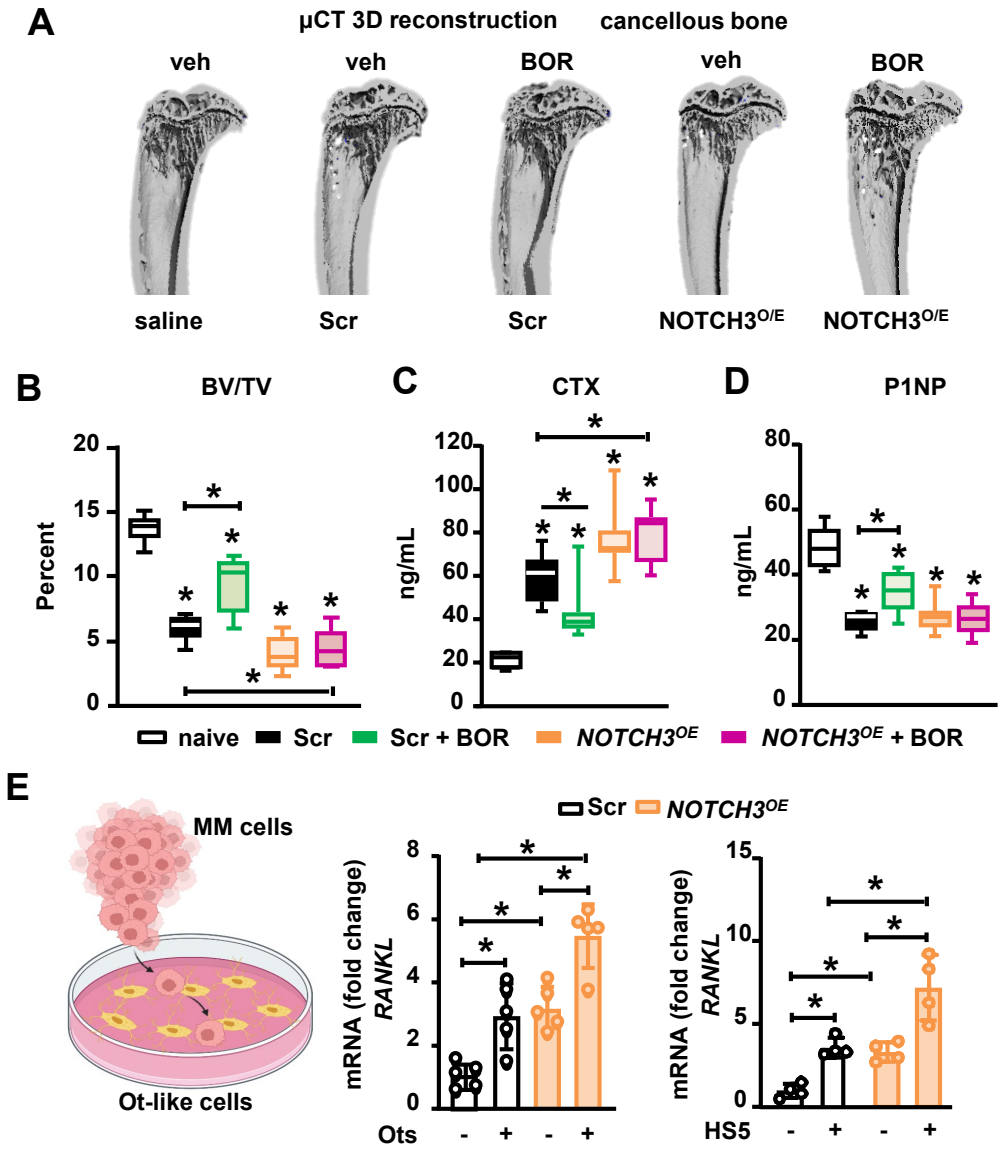

Supplementary Figure 6. *NOTCH3* activation in MM cells impedes the beneficial effects of BOR on bone. (A) Representative microCT 3D reconstruction images of tibiae, (B) tibiae cancellous bone volume/tissue volume (BV/TV) quantification, serum CTX (C), and P1NP (D) in mice injected with Scramble (Scr) or *NOTCH3* activated (*NOTCH3*^{OE}) MM cells and treated with/without Bortezomib (BOR). N=6-11 mice/group. *p<0.05 vs. saline by One-way ANOVA, followed by a Tukey post hoc test. Boxes show the data interquartile range, the middle line in the box represents the median, and whiskers the 95% confidence interval of the mean. (B, C, D). (E) *RANKL* gene expression in Scr or *NOTCH3*^{OE} MM cells co-cultured with osteocytes (Ots) or stromal cells (HS5). N=4/group. *p<0.05 by Two-way ANOVA, followed by a Tukey post hoc test. Representative experiments out of two are shown (E). Data are shown as mean ± SD; each dot represents an independent sample (E).

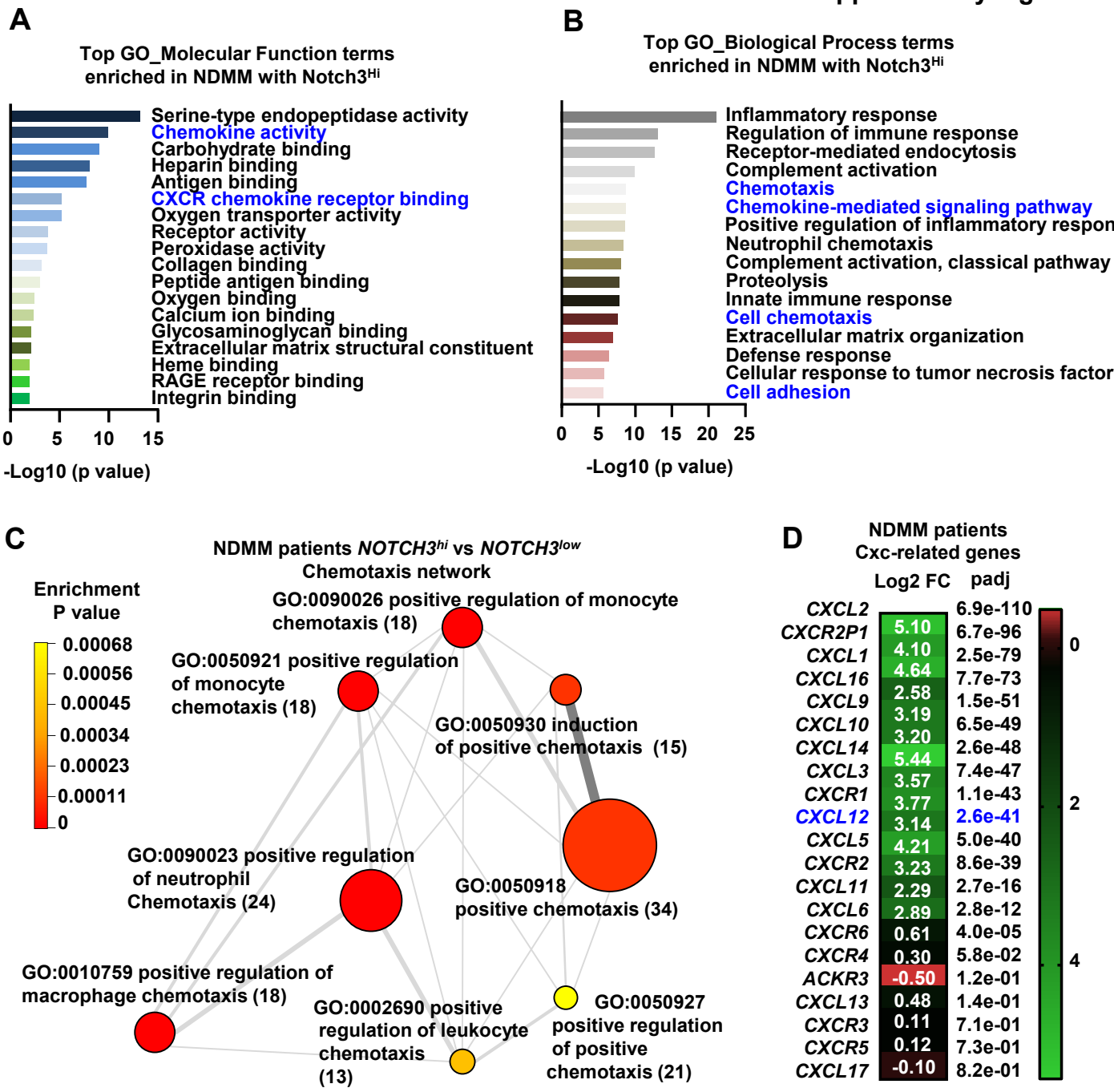

Supplementary Figure 7. Gene expression and GO term bioinformatics differential analysis in newly diagnosed patients with high vs. low *NOTCH3* expression. Gene ontology (GO) analysis of upregulated genes in *NOTCH3* high vs. low newly diagnosed MM (NDMM) patients. Bar charts showing the top 20 GO terms for Molecular Function (A) and Biological Process (B) ranked by p-value. N=768 patients. (C) Network plot of selected upregulated functional enrichment analysis of GO terms related to Chemotaxis in NDMM patients with high vs. low NOTCH3 expression. The size of the circles represents the number of genes in the individual GO terms. N=768 patients. The thickness of the lines represents the number of overlapped genes between the individual GO terms. (D) Differentially expressed CXC-related genes and the corresponding fold changes and adjusted p values in NDMM patients with high vs. low *NOTCH3* expression by Student's t-test. N=768 patients.

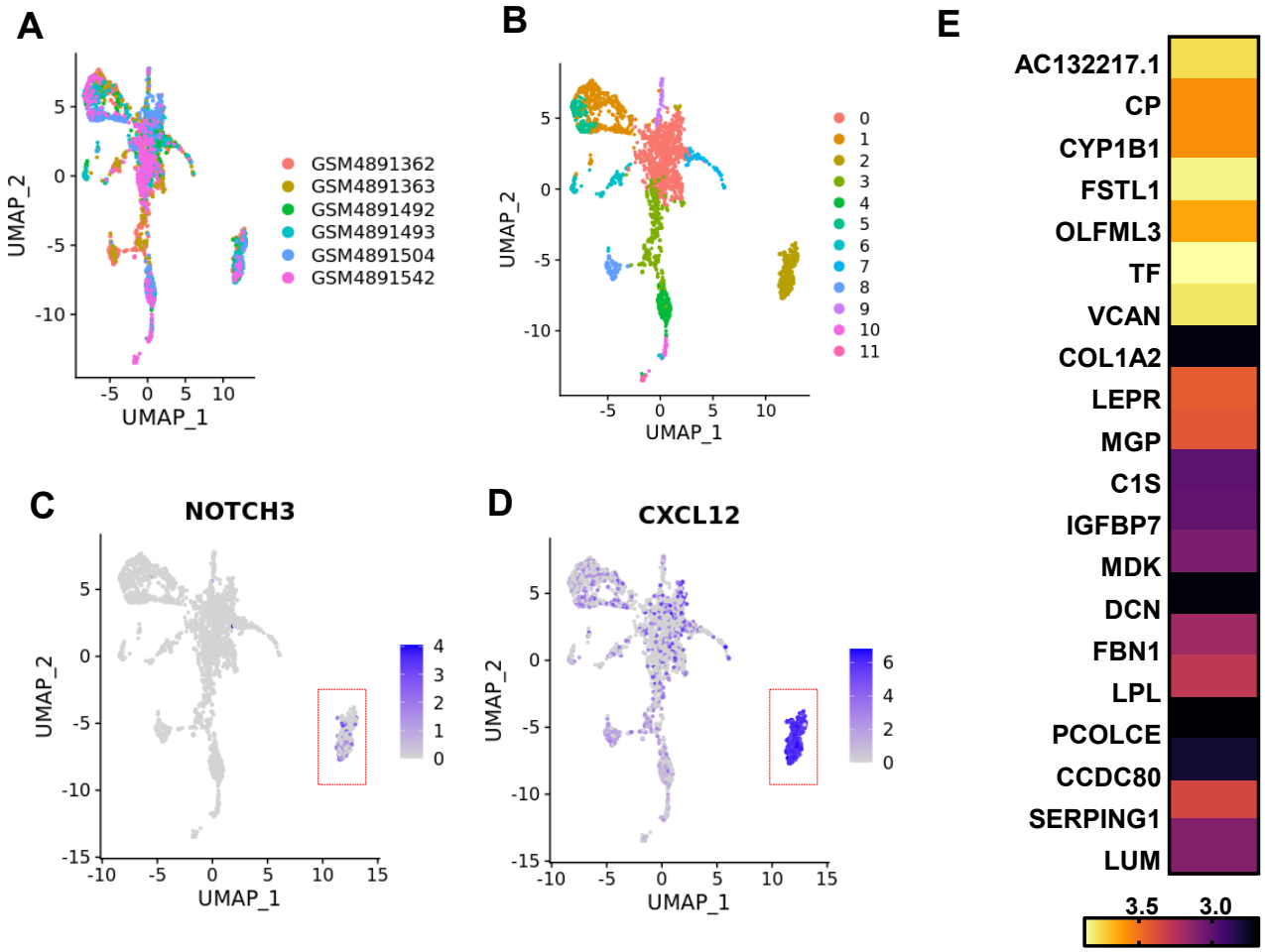

F

GEO_Accession (exp)	Replicate_ ID	Sample Name	source_name	SRA Study	Time_ point	disease_ state	Organ	SAMPLE_TYPE	selection_ marker	Cohort
GSM4891362	Kydar04	GSM4891362	Bone marrow aspiration	SRP292331	Baseline	PRMM	Bone marrow	Bone marrow aspiration	CD138+/CD38+	Refractory
GSM4891363	Kydar04	GSM4891363	Bone marrow aspiration	SRP292331	Baseline	PRMM	Bone marrow	Bone marrow aspiration	CD138+/CD38+	Refractory
GSM4891492	Kydar07_Post2	GSM4891492	Bone marrow aspiration	SRP292331	Cycle 10	PRMM	Bone marrow	Bone marrow aspiration	CD138+/CD38+	
GSM4891493	Kydar07_Post2	GSM4891493	Bone marrow aspiration	SRP292331	Cycle 10	PRMM	Bone marrow	Bone marrow aspiration	CD138+/CD38+	
GSM4891504	Kydar29_Post	GSM4891504	Bone marrow aspiration	SRP292331	Cycle 4	PRMM	Bone marrow	Bone marrow aspiration	CD138+/CD38+	
GSM4891542	Kydar15_Post2	GSM4891542	Bone marrow aspiration	SRP292331	Cycle 10	PRMM	Bone marrow	Bone marrow aspiration	CD138+/CD38+	

Supplementary Figure 8. Identification of a population of CD138$^+$ cells co-expressing *NOTCH3* and *CXCL12* in RRMM patients. Single-cell RNA-seq analysis, UMAP-based visualization of major classes of CD138$^+$ cells based on a published single-cell RNA sequencing dataset and colored by patient (A) or cluster (B). Gene expression plot of *NOTCH3* (C) and *CXCL12* (D) of individual CD138$^+$ cells on UMAP coordinates. (E) Top 20 most upregulated genes in cluster 2 containing *NOTCH3*$^+$-*CXCL12*$^+$ MM cells. (F) Patient and scRNAseq data characteristics.

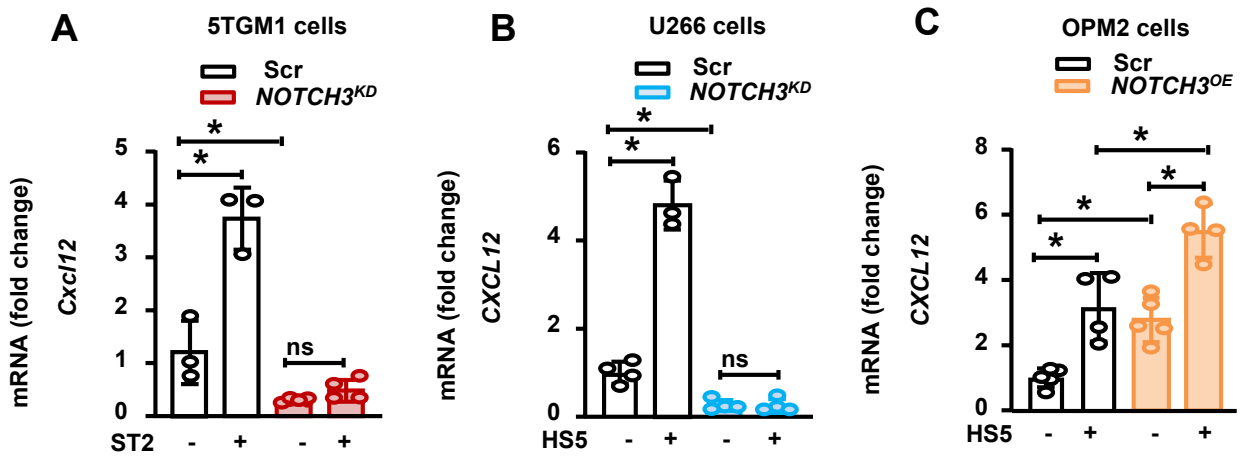

Supplementary Figure 9. Stromal cell-mediated NOTCH3 signaling regulates *CXCL12* expression in MM cells. mRNA expression of *CXCL12* in (A) 5TGM1 Scramble (Scr) and *NOTCH3* knockdown (*NOTCH3*^{KD}), (B) U266 Scr and *NOTCH3*^{KD}, and (C) OPM2 Scr and *NOTCH3* activated (*NOTCH3*^{OE}) MM cells cultured for 48h in the absence and presence of stromal cells. ST2: murine stromal cells; HS-5: human stromal cells. N=4/group. *p<0.05 by Two-way ANOVA, followed by a Tukey post hoc test. ns: non-significant. Data are shown as mean ± SD; each dot represents an independent sample. Representative experiments out of two are shown.

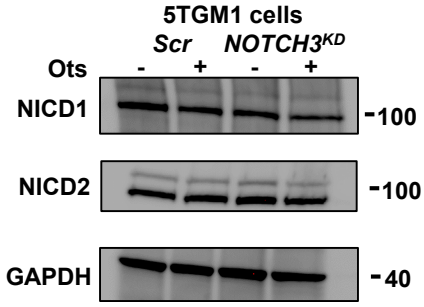

Supplementary Figure 10. Osteocytes do not activate NOTCH1 or NOTCH2 in MM cells. Cleaved NOTCH1 and 2 intracellular domain (NICD) protein levels in murine Scramble (Scr) or *NOTCH3* knockdown (*NOTCH3*^{KD}) 5TGM1 MM cells culture alone or with osteocytes (Ots).

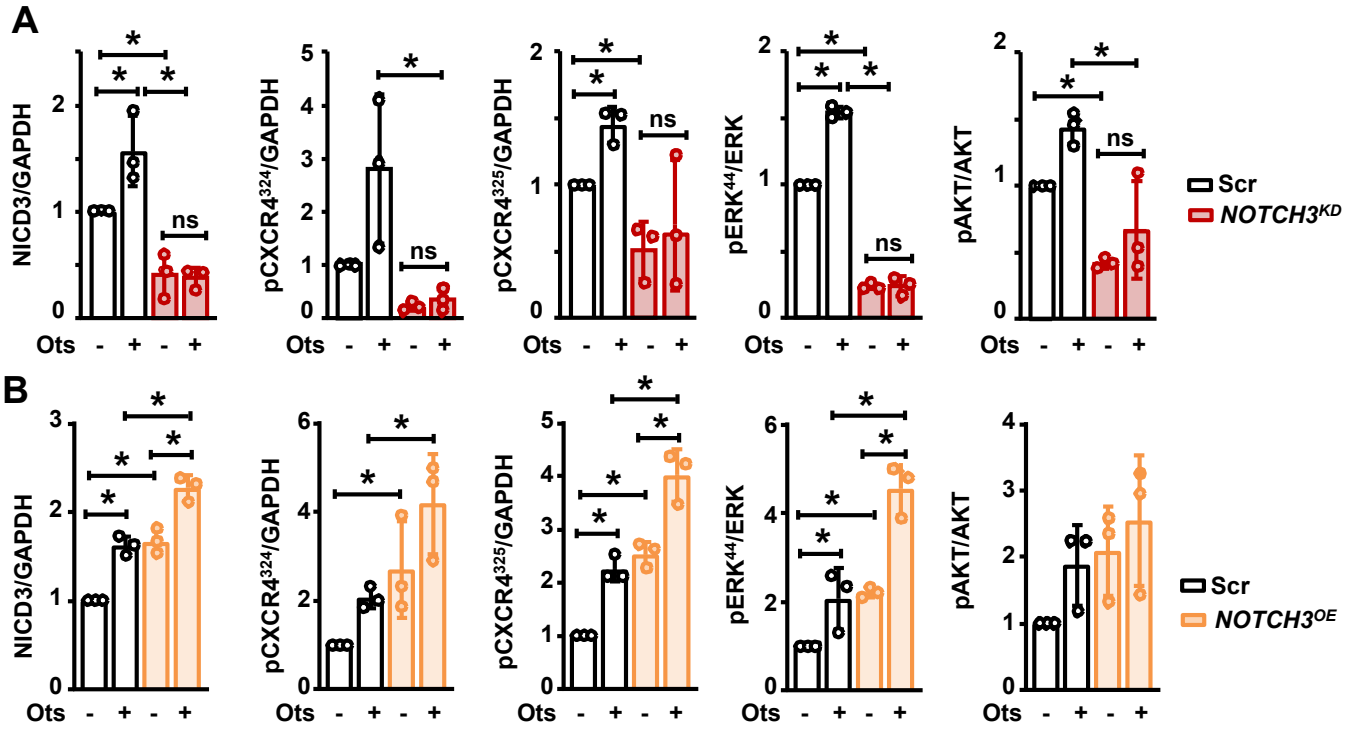

Supplementary Figure 11. Osteocyte-mediated NOTCH3 signals activate CXCR4 signaling via AKT and ERK phosphorylation. Quantification of three independent western blots from experiments displayed in Figure 6 A-B using (A) Scramble (Scr) and *NOTCH3* knockdown (*NOTCH3*^{KD}) 5TGM1 and (B) Scr and *NOTCH3* activated (*NOTCH3*^{OE}) OPM2 MM cells co-cultured in the absence/presence of osteocytes (Ots). N=3/group. *p<0.05 Two-Way ANOVA, followed by a Tukey post hoc test. Data are shown as mean ± SD; each dot represents an independent sample.

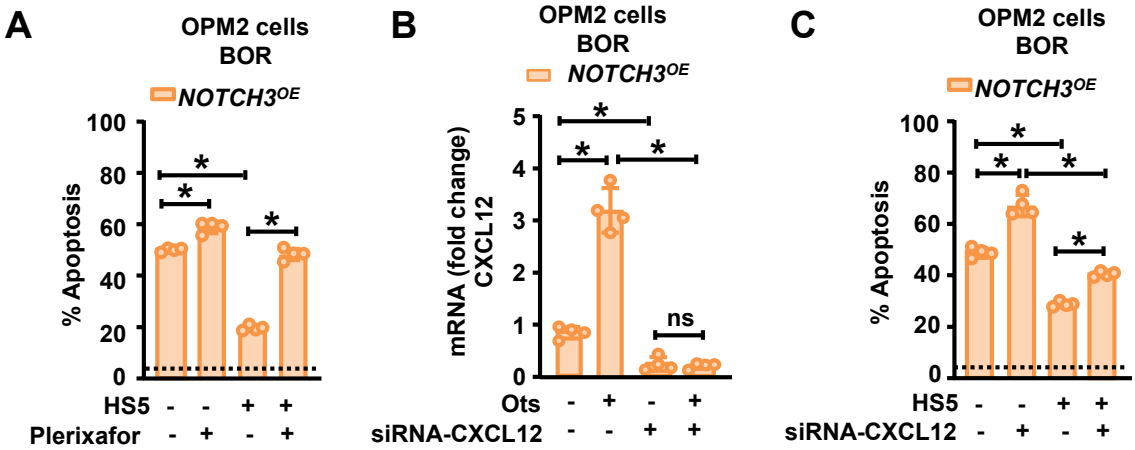

Supplementary Figure 12. Genetic or pharmacologic inhibition of CXCL12 signaling prevents stroma-mediated drug resistance to Bortezomib-based therapies. (A) Percent apoptosis in *NOTCH3* activated (*NOTCH3*^{OE}) OPM2 MM cells treated with Bortezomib (BOR) in the presence/absence of Plerixafor and cultured with/without osteocytes (Ots). N=4/group; BOR=48h. *p<0.05 by Two-Way ANOVA, followed by a Tukey post hoc test. (B) *CXCL12* gene expression in *NOTCH3*^{OE} OPM2 MM cells treated with/without siRNAs against *CXCL12* and cultured alone or with Ots. N=4; *p<0.05 by Two-way ANOVA, followed by a Tukey post hoc test. (C) Percent apoptosis in *NOTCH3*^{OE} OPM2 MM cells treated with BOR in the presence/absence of *siRNA-CXCL12* and cultured with/without Ots. N=4/group; BOR=48h. *p<0.05 by Two-Way ANOVA, followed by a Tukey post hoc test. Data are shown as mean ± SD; each dot represents an independent sample. Dotted line represents the percent apoptosis in vehicle-treated OPM2 MM cells cultured alone. siRNA: small interference RNA. Representative experiments out of two are shown.

Supplementary methods.

Reagents. RPMI 1640 media, Minimum Essential Media (MEM) α, fetal bovine serum, bovine calf serum, Normocin, antibiotics (penicillin/streptomycin), TriZol, and DiI/DiD cell trackers were purchased from Invitrogen Life Technologies (Grand Island, NY, USA). Trypan Blue was purchased from Sigma Aldrich (St. Louis, MO, USA). γ-secretase inhibitor XX (GSI-XX) was purchased from Calbiochem (San Diego, CA, USA). Anti-GAPDH (Cat#2118S, RRID: AB_561053), anti-NOTCH1 (Cat #4380S, RRID: AB_10691684), anti-NOTCH2 (Cat #5732S, RRID: AB_10693319), anti-p-ERK (Cat#9101, RRID: AB_331646), anti-ERK (Cat#9102, RRID: AB_330744), anti-pAKT (Cat# 4060S), and anti-AKT (Cat# 9272S) antibodies were purchased from Cell Signaling Technologies (Danvers, MA, USA); anti-NOTCH3 (ab23426, RRID: AB_776841), anti-NOTCH4 (ab166605), and anti-pCXCR4 (ab74012, RRID: AB_1523429) antibodies were purchased from Abcam (Cambridge, MA, USA). Plerixafor (Cat#S8030), Bortezomib (Cat#S1013), and Lenalidomide (Cat#S1029) were purchased from Selleckchem (Houston, TX, USA); Dexamethasone (Cat#D4902) was purchased from Sigma (St. Louis, MO, USA); and *CXCL12* siRNA (Cat#SR304303) was purchased from Origene Technology (Rockville, MD, USA). Puromycin (Cat#58-58-2) and Blasticidin (Cat#ant-bl) were purchased from InvivoGen (San Diego, CA, USA).

Cell culture. 5TGM1 murine MM cells (RRID: CVCL_VI66) were obtained from Dr. B. Oyajobi (University of Texas at San Antonio, TX, USA), and MLO-A5 murine osteocyte-like cells (RRID: CVCL_0P24) were purchased from Kerafast (Boston, MA, USA). OPM2 (RRID: CVCL_1625) and U266 (RRID: CVCL_0566**)** human MM cells were obtained from Dr. G. D. Roodman (Indiana University, IN, USA). ST2 murine stromal cells (RRID: CVCL_2205) were obtained from Dr. Jin-Ran Chen (University of Arkansas for Medical Sciences, AR, USA), and HS-5 human stromal

cells (RRID: CVCL_3720) were purchased from ATCC (Manassas, VA, USA). Cell lines were checked for mycoplasma weekly and routinely examined for proper morphology, population doubling, and paraprotein production. MM cell lines (5TGM1, OPM2, U266) were cultured in RPMI with 10% FCS and 1% P/S. Osteocyte-like cells (MLOA5) were cultured on calf skin collagen type I-coated plates in αMEM media with 2.5% FBS, 2.5% BCS, and 1% P/S. Stromal cells (ST2, HS5) were cultured in DMEM with 10% FBS and 1% P/S.

Gene Expression. Total RNA was isolated from MM cells and bone tissues using Trizol and converted to cDNA (Invitrogen Life Technologies), following the manufacturer's directions. EDTA incubations were used to separate MM cells from the osteocytes/stroma, as previously described.[1, 2] Gene expression was quantified by quantitative real-time PCR (qPCR) using TaqMan assays from Applied Biosystems (Foster City, CA, USA), following the manufacturer's directions. Gene expression levels were calculated using the comparative threshold (CT) method and were normalized to the housekeeping gene GAPDH.[1, 2]

Western Blot. Cell lysates (50μg) were boiled in the presence of SDS sample buffer (NuPAGE LDS sample buffer; Invitrogen) for 10 minutes and subjected to electrophoresis on 10% SDS-PAGE (Bio-Rad Laboratories). Proteins were transferred to PVDF membranes using a semidry blotter (Bio-Rad) and incubated in a blocking solution (5% nonfat dry milk in TBS containing 0.1% Tween-20) for 1 hour to reduce nonspecific binding. Immunoblots were performed using anti-GAPDH, pCXCL12, AKT, pAKT, ERK, pERK, NOTCH1, NOTCH2, and NOTCH3 antibodies (1:1000) followed by goat anti-rabbit secondary antibodies, conjugated to horseradish peroxidase (1:2000) in 5% milk (Santa Cruz Biotechnology). Western blots were developed using an enhanced chemiluminescence detection assay following the manufacturer's directions (Bio-Rad). Protein bands were quantified using ImageJ.

Enzyme-linked immunoassays (ELISA). The levels of the tumor biomarkers human lambda (Bethyl Laboratories; Cat#E88-116) or IgG2B (Invitrogen; Cat#88-50430-88) paraproteins produced by OPM2/U266 and 5TGM1 cells, respectively, were used to determine tumor growth/burden in vivo (serum) and ex vivo (conditioned media). The bone resorption biomarker C-telopeptide of type 1 collagen (CTX) (Immunodiagnosticsystems; Cat#AC-06F1) and bone formation marker propeptide of type 1 collagen (P1NP) (Immunodiagnosticsystems; Cat#AC-33F1) were analyzed in serum (*in vivo*). Tumor growth/burden, bone resorption, and bone formation were determined using commercially available specific ELISA and following the manufacturer's recommendations.

Apoptosis and proliferation assays. Apoptosis in MM cells was assessed by flow cytometry using the FITC (OPM2 or U266) or PerCP-Cyanine5.5 (5TGM1) Annexin V apoptosis Detection kit (BD Biosciences) following the manufacturer's recommendations. For analysis of apoptosis in co-cultures, OPM2 cells were selected by using mCherry fluorescence, and 5TGM1 and U266 cells were stained with the fluorescent cell-tracker DiD before plating cells (emission 665 nm; excitation 645 nm) following the manufacturer's recommendations. Samples were analyzed in a BD FACSCalibur (UAMS Core Facility for Flow cytometry) within 1h. At least 10,000 cells were used for each group, and the data were analyzed by FlowJo software to detect different cell populations. Co-cultures were treated with Plerixafor (25uM), BOR (3nM), VRd (BOR: 2nM, Lenalidomide: 1uM, Dexamethasone: 10nM) were refreshed every 24h. OPM2 cells were stained with a fluorescent cell tracker DiI before plating cells following the manufacturer's recommendations for proliferation analysis. After 48h of culture, cells were collected, re-suspended in PBS, and DiI fluorescence was read at 520 to 565 nM on a plate reader.

Genetic inhibition/activation in MM cells. Control and *NOTCH3* knockdown 5TGMI MM cells were generated as described before.[2] To generate stable control and *NOTCH3*-activated OPM2 MM cells, we first transduced cells with CRISPRa dCas9-VP64 lentiviral particles (MOI=10; Addgene, Watertown, MA, USA) and treated them with Blasticidin (5ug/mL) for selection. OPM2 MM cells stably expressing CRISPRa dCas9-VP64 were transduced with lentiviral particles carrying scramble or NOTCH3 directed sgRNAs (TCCGCGCGTCCCAGGCTGTG) and mCherry (MOI=10; Genecopoeia, Rockville, MD. USA) and treated with Puromycin (1ug/mL) for selection. To generate control and *NOTCH3* knockdown U266 MM cells, cells were transduced with a plasmid containing a sgRNA sequence against NOTCH3 cloned into a guide RNA Cas9 vector (a gift from Dr. Helena Karlström, Karolinska Institutet, Sweden)[3] and treated with Puromycin (3ug/mL) for selection. 5TGM1 transduced MM cells were maintained in complete media supplemented with 3ug/mL of Puromycin, OPM2 cells were maintained in complete media supplemented with 0.5ug/mL Puromycin and 2.5 μg/mL Blasticidin, and U266 cells were maintained in complete media supplemented with 1.5ug/mL Puromycin. To transiently inhibit CXCL12 in MM cells, we treated OPM2 MM cells with 1.0 nM of siRNA against CXCL12 for 24h before establishing MM-osteocyte/stroma co-cultures.

Ex vivo organ cultures. Ex vivo MM-murine bone organ cultures were established with calvarial bones from NOD.Cg-Prkdcscid Il2rgtm1Wjl/SzJ (NSG; Jackson's Lab, strain: 005557) for human U266 or OPM2 MM cells or with calvarial bones from C57BL/KaLwRijHsd mice of murine 5TGM1 MM cells, as described before.[1] For these ex vivo cultures, $5x10^4$ MM cells were plated on calvarial bones, and $2x10^5$ MM cells were plated on human bones. The human bone samples were obtained from 2 males, with no pathologies or medications that could affect bone mass or architecture. Treatments (Plerixafor 50uM; BT-GSI 10 uM; BOR 3nM; VRd: BOR 2nM,

Lenilidomide 1uM, Dexamethasone 10nM) were refreshed every 3 days. 50% of conditioned media was collected and replaced after 4 days of culture. All conditioned media was collected after 11 days of culture. Tumor growth was quantified by luciferase activity or ELISA.

Bioinformatic analyses. We segregated high vs. low *NOTCH3* patients using quartile measures and performed comparative gene expression analysis as described before.[2] The gene list for the GSEA on responses to BOR was constructed using data from Mulligan et al.[4] Samples were classified as progressive/relapsed if they met two criteria: i) the patient must have a baseline sample, and ii) the patient must have a sample taken after either a complete or partial response. The scRNASeq analysis was conducted on data previously published by Cohen et al. (GSE161195).[5] Salmon gene count data were imported into and normalized using the R package DESeq2. Differential expression analysis of *NOTCH3* high versus low samples was performed using DESeq2, with an adjusted p-value cutoff of 0.05. Gene set enrichment analysis was then conducted using the R package fgsea.[6] Survival analyses were performed and visualized in R using the survival and survminer packages. Comparison of gene expression between NDMM (n=768) and paired NDMM vs. progression/relapsed (PRMM; n=70) samples was performed and visualized using the R package ggpubr. Correlation analysis between *CXCL12* and *NOTCH3* was performed in both the NDMM and progressive/relapsed samples using the R package ggpubr. Mutation data for *NOTCH3* was obtained from the MMRF Researcher Gateway for corresponding whole-exome sequencing samples (n=725). All single-cell analyses were performed using the R package Seurat as described before.[7] The PIANO package was used to perform the gene-set enrichment analysis of Gene Ontology (GO) and gene networks using adjusted *p*-value and log2 fold changes as the input to calculate the enrichment p-value of the GO terms.[8] For human cell line mutation analysis, the (HMCL69_Preliminary_Mutations_Samtools.xlsx) file was utilized to

determine which cell lines were mutated for NOTCH3, which was downloaded from the Keats Lab repository (https://www.keatslab.org).

References

1. Delgado-Calle J, Anderson J, Cregor MD, et al. Bidirectional Notch Signaling and Osteocyte-Derived Factors in the Bone Marrow Microenvironment Promote Tumor Cell Proliferation and Bone Destruction in Multiple Myeloma. Cancer Res. 2016;76(5):1089-1100.
2. Sabol HM, Amorim T, Ashby C, et al. Notch3 signaling between myeloma cells and osteocytes in the tumor niche promotes tumor growth and bone destruction. Neoplasia. 2022;28(100785.
3. Wu D, Wang S, Oliveira DV, et al. The infantile myofibromatosis NOTCH3 L1519P mutation leads to hyperactivated ligand-independent Notch signaling and increased PDGFRB expression. Dis Model Mech. 2021;14(2):
4. Mulligan G, Mitsiades C, Bryant B, et al. Gene expression profiling and correlation with outcome in clinical trials of the proteasome inhibitor bortezomib. Blood. 2007;109(8):3177-3188.
5. Cohen YC, Zada M, Wang SY, et al. Identification of resistance pathways and therapeutic targets in relapsed multiple myeloma patients through single-cell sequencing. Nat Med. 2021;27(3):491-503.
6. Korotkevich G, Sukhov V, Budin N, Shpak B, Artyomov MN, Sergushichev A. Fast gene set enrichment analysis. bioRxiv. 2021;060012.
7. Satija R, Farrell JA, Gennert D, Schier AF, Regev A. Spatial reconstruction of single-cell gene expression data. Nat Biotechnol. 2015;33(5):495-502.

8. Patro R, Duggal G, Love MI, Irizarry RA, Kingsford C. Salmon provides fast and bias-aware quantification of transcript expression. Nat Methods. 2017;14(4):417-419.

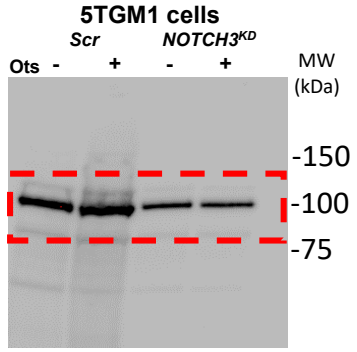

NICD3
(Abcam ab23426)

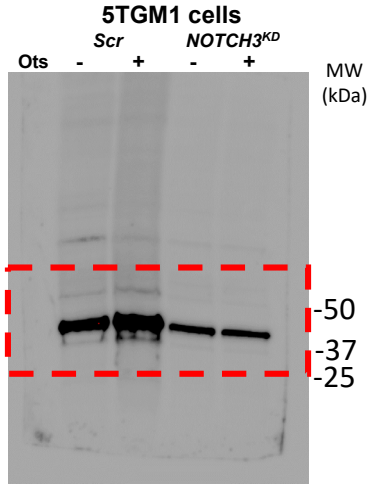

pCXCR4
(Abcam ab74012)

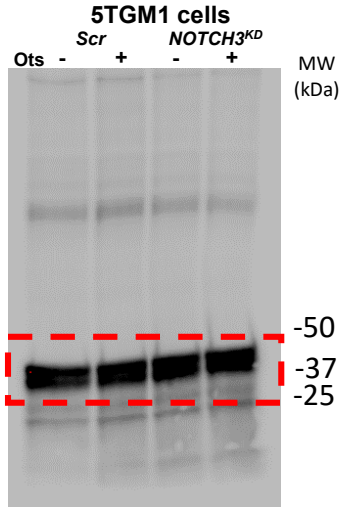

GAPDH
(Cell signaling 14C10)

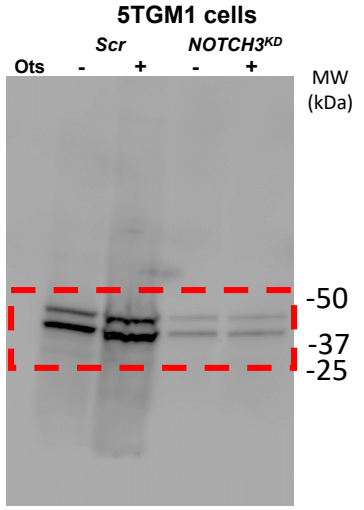

pERK
(Cell signaling 9101)

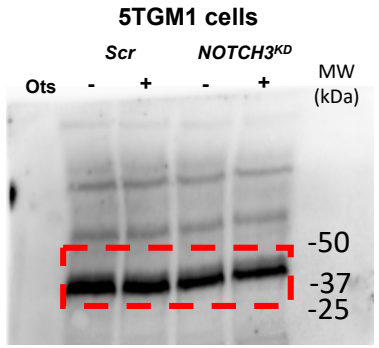

ERK
(Cell signaling 9102)

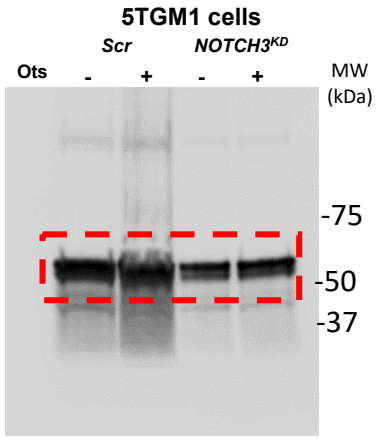

pAKT
(Cell signaling S473)

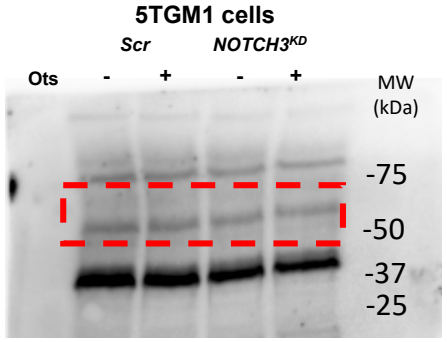

AKT
(Cell signaling 9272S)

Figure 6A

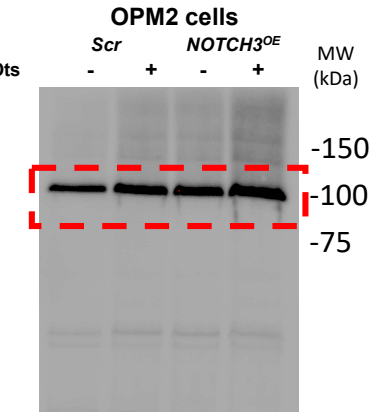

NICD3
(Abcam ab23426)

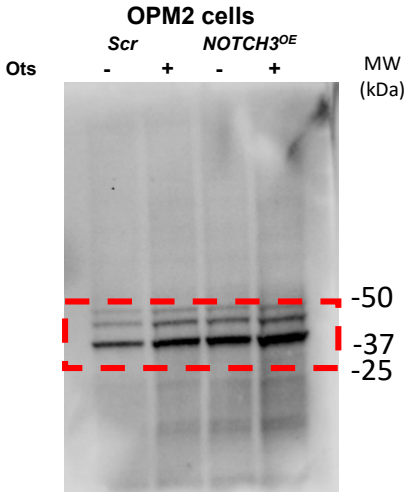

pCXCR4
(Abcam ab74012)

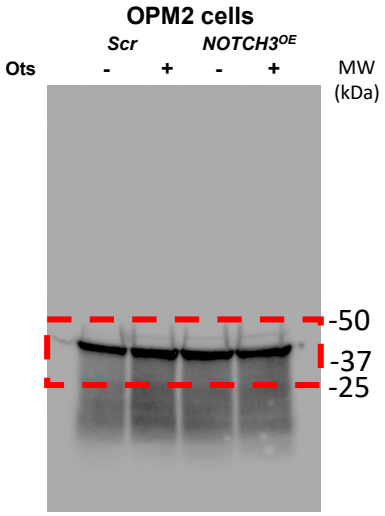

GAPDH
(Cell signaling 14C10)

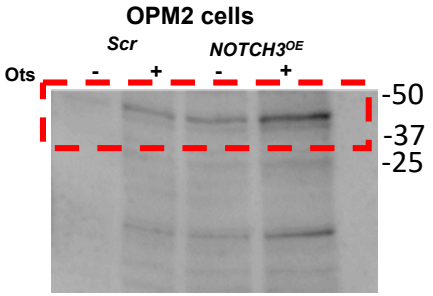

pERK
(Cell signaling 9101)

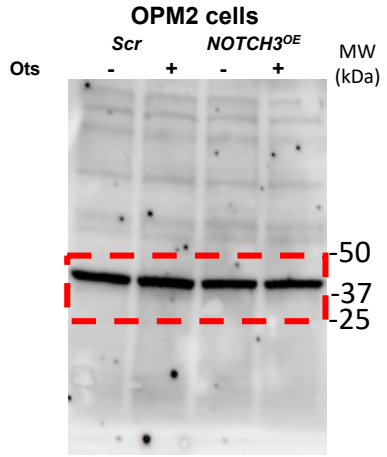

ERK
(Cell signaling 9102)

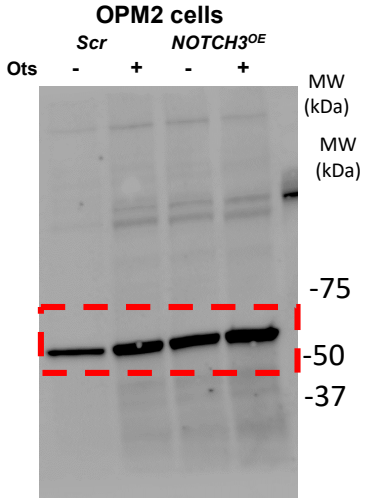

pAKT
(Cell signaling S473)

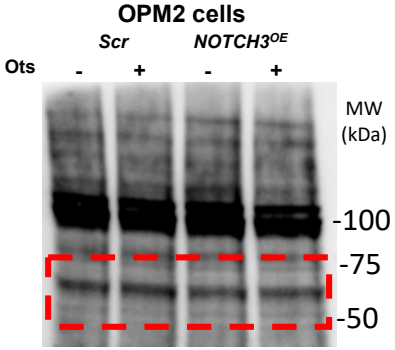

AKT
(Cell signaling 9272S)

Figure 6B

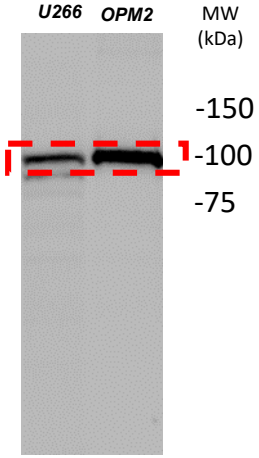

Notch1
(Cell signaling D6F11)

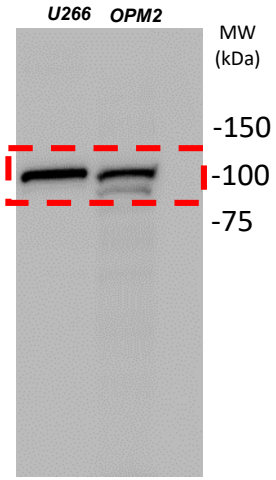

Notch2
(Cell signaling D76A6)

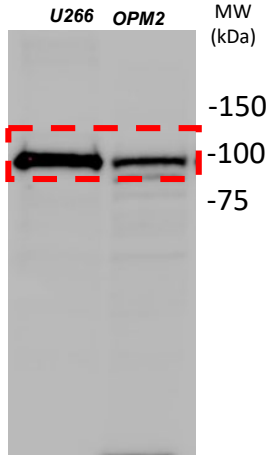

Notch3
(Abcam ab23426)

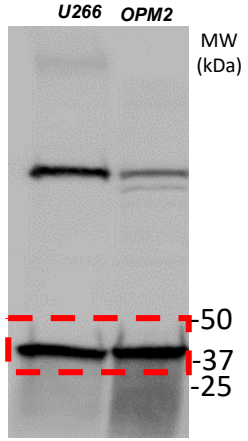

Gapdh
(Cell signaling 14C10)

Supp. Fig 3a

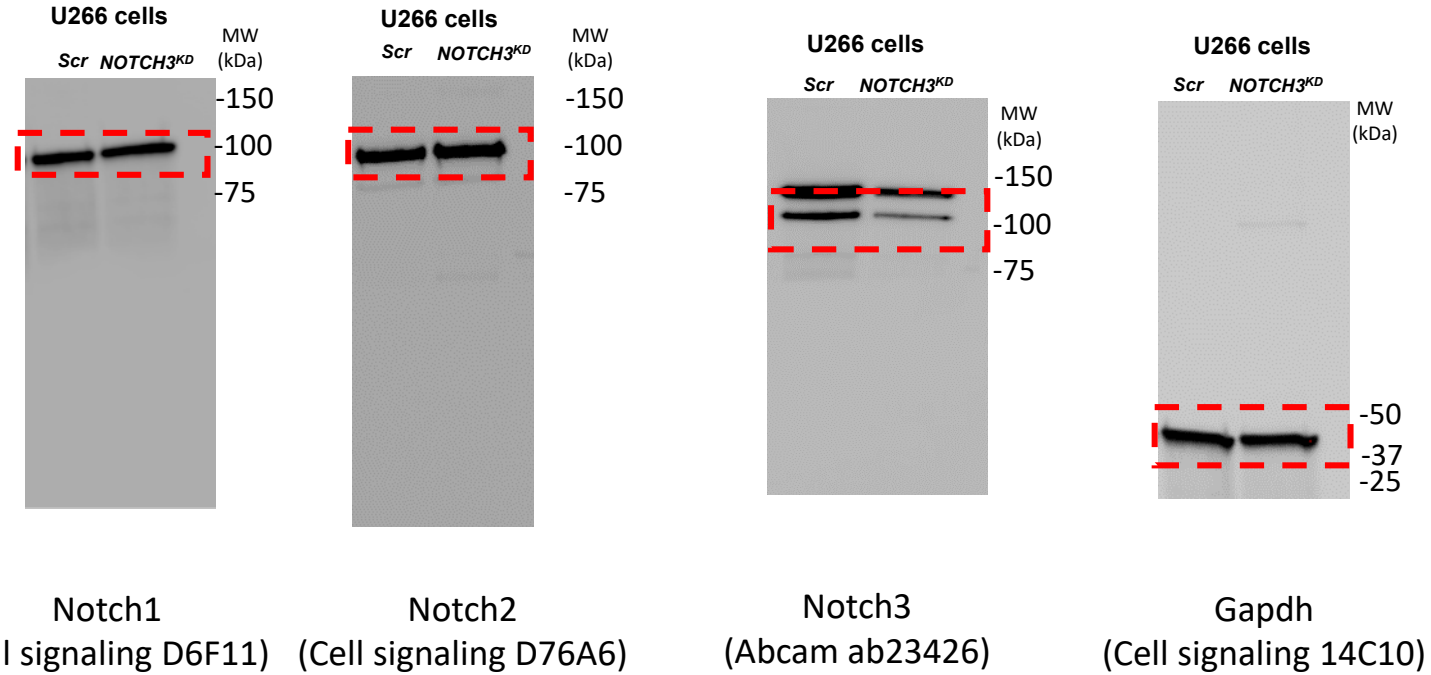

Notch1
(Cell signaling D6F11)

Notch2
(Cell signaling D76A6)

Notch3
(Abcam ab23426)

Gapdh
(Cell signaling 14C10)

Supp. Fig 3b

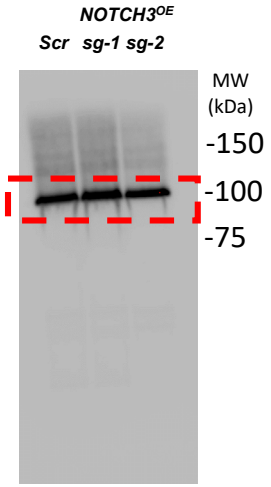

Notch1
(Cell signaling D6F11)

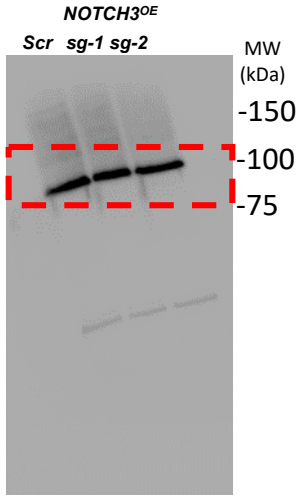

Notch2
(Cell signaling D76A6)

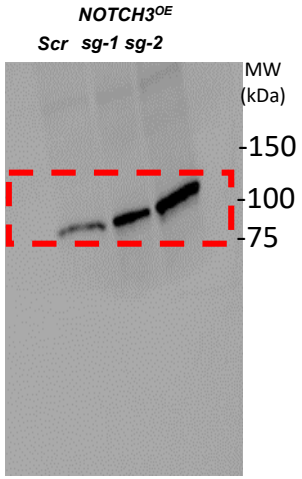

Notch3
(Abcam ab23426)

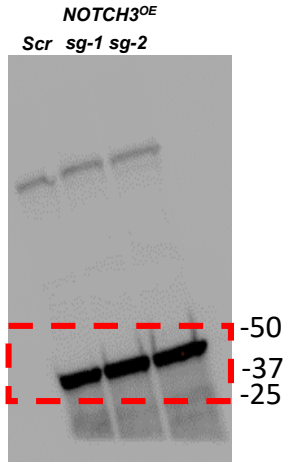

Gapdh
(Cell signaling 14C10)

Supp. Fig 3c

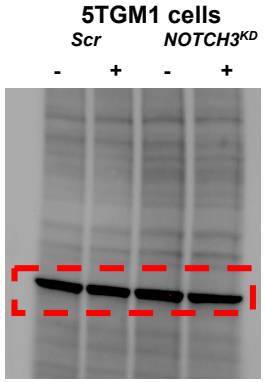

Gapdh
(Cell signaling 14C10)

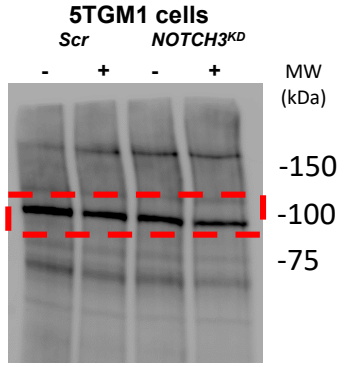

Notch1
(Cell signaling D6F11)

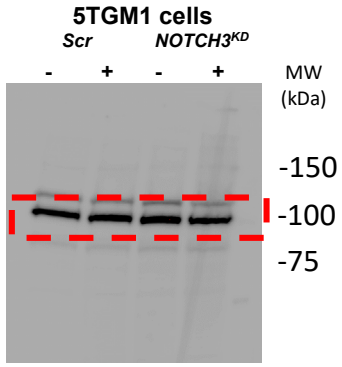

Notch2
(Cell signaling D76A6)

Supp. Fig 10